PROCEEDINGS, 51st Workshop on Geothermal Reservoir Engineering
Stanford University, Stanford, California, February 9-11, 2026
SGP-TR-230

Reservoir Engineering Characteristics of Geothermal Permeability Regimes

John F. Murphy and Ryan B. Libbey

Ormat Technologies, Inc. 6884 Sierra Center Pkwy, NV, USA 89511

jmurphy@ormat.com

Keywords: Reservoir Engineering, Productivity Index, Permeability, Capacity Estimation, Temperature Decline, Analog Study

ABSTRACT

Geothermal systems occur across diverse geologic settings and the viability of a conventional development depends not only on elevated temperatures, which are essential, but also on the distribution of permeable rocks and fractures that enable sustained fluid production. Observations and analysis from global analogs reveal characteristic pressure and temperature behaviors that allow reservoirs to be classified by permeability type. This classification enhances early assessments of resource potential and informs exploration and development strategies. The characteristics of four end-member Permeability Regimes are described: Discrete, Limited Distributed, Enhanced Distributed, and Stratigraphic. A companion study, Libbey and Murphy (2026), provides greater detail on the geology of these regimes and resource parameters of Area and Thickness which characterize these systems as well as detailing a standardized methodology utilizing these characteristics for estimating resource capacity.

1. INTRODUCTION

Geothermal reservoirs can be characterized by their geologic/spatial characteristics (Libbey and Murphy, 2026) and by their reservoir engineering characteristics. Reservoir engineering characteristics include individual well permeability (productivity/injectivity index), the feedzone distribution, reservoir permeability-thickness, inter-well connections (e.g. tracer returns), and development metrics such as pressure response, temperature/enthalpy response, and per-well generation output. A global survey of geothermal systems suggests that geothermal permeability types can be categorized into four regimes: (1) Discrete, (2) Limited Distributed, (3), Enhanced Distributed, and (4) Stratigraphic. Low permeability reservoirs, which may be candidates for hydraulic stimulation (EGS) are not considered in this categorization but may be considered a low permeability endmember of Limited Distributed or Stratigraphic systems. Figure 1 provides a schematic depiction of these Permeability Regimes and characteristics of each.

Fundamentally, these categories describe a distribution of permeability on a spectrum, where Discrete systems have very low (negligible) background permeability and flow is dominated by permeability at localized zones of elevated fracture density, typically at structural discontinuities. Limited Distributed systems, conversely, are dominantly background fractures, the cumulative volume of which contribute to permeability. If a system with distributed background permeability also hosts larger fractures or faults with enhanced permeability, the system should be categorized as Enhanced Distributed. Stratigraphic systems contain stacked sedimentary sequences of variable permeability, with the permeability of these systems dominantly in the matrix pore space.

Identifying the permeability regime of a system is useful to predict the power generating potential of that reservoir and to guide the exploration and development strategy by setting expectations for well performance and inter-well interactions. Temperature is an independent variable of these permeability types and not a determining factor in categorizing a system under this schema, but the commercial potential of a system is highly dependent on the temperature. Sixty-five geothermal fields were characterized for this study and are referenced throughout.

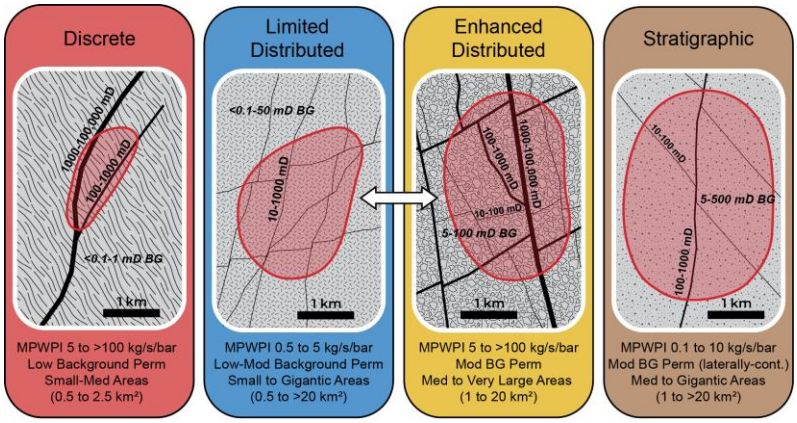

Figure 1: Plan-View Generalized Schematics of the Four End-Member Permeability Regimes of Geothermal Systems with Representative Ranges of Background and Fracture Permeability (Reproduced from Libbey and Murphy, 2026)

2. PRODUCTIVITY INDEX RANGES FOR PERMEABILITY REGIMES

Productivity Index (PI) is defined as the change in pressure at the center of permeability in a well for a given change in flow rate in that well alone. In high permeability formations, pressure will stabilize relatively quickly (matter of minutes to days), but lower permeability formations will decline more gradually over a timeframe of weeks or months (Sanyal and Butler, 2010). For the purposes of this characterization, productivity index is calculated at the stabilized condition, with the acknowledgement that precise quantification is often difficult with varying operating parameters. PI is highly dependent on fluid properties, in particular temperature/enthalpy, and especially dynamic in two-phase feedzones and reservoirs (Pasikki 2017). The study herein does not normalize PI to account for these enthalpy effects, instead using the demonstrated operating PI in units of kg/s/bar where possible. In using this formulation, care must be taken to recognize that the relationship between injectivity index (II), PI for liquid feedzones, and PI for two-phase or dry-steam feedzones is complex, and in practical terms the PI can be greatly reduced if two-phase conditions are encountered, due to the combined effects of lower density and relative permeability decreasing mobility.

The median of available production well PIs (MPWPI) on a given field was used to characterize that field throughout this paper, shown in Figure 2 for analogs representing each permeability regime with characterizing statistics summarized in Table 1 and individual field details provided in Table 4 to Table 7. MPWPIs for the studied Discrete system calibration analogs range from 7.1 to 377 kg/s/bar, and the median across all Discrete fields is 39 kg/s/bar. Among the Discrete systems characterized, most are found in the Great Basin region of the United States, with Puna in Hawaii, USA and Platanares in Honduras representing systems outside that region.

Likely the most common Permeability Regime worldwide is the Limited Distributed type, which is characterized by median PIs in the range of 0.5 to 5 kg/s/bar, with a median of 1.6 kg/s/bar in the fields characterized herein. As seen in Figure 2, individual wells may fall outside this range (up to 20 kg/s/bar in the fields characterized), but the overall development (median producer) is primarily from wells with lower productivity. Limited Distributed systems occur across a wide range of temperatures (from 130 °C at Raft River to exceeding 330 °C at Ijen). They also occur in diverse geologic settings, including volcanic arcs, zones of regional continental extension, and hot spot volcanoes (Libbey and Murphy, 2026). The two dry steam fields characterized, The Geysers, California USA and Kamojang, Java, Indonesia, are both examples of limited distributed fields, with estimated MPWPIs of 3 and 1.5 kg/s per bar, respectively.

Enhanced Distributed systems start where Limited Distributed systems end, extending from 5 kg/s/bar up to a field median over 100 kg/s/bar at Steamboat in Nevada, USA, Cove Fort in Utah, USA, and the Don A. Campbell field in Nevada, USA. The median of the MPWPI among the studied Enhanced Distributed calibration analogs is 14.5 kg/s/bar. In Enhanced Distributed systems, permeability is contained both in minor fractures and background permeability (including those that could comprise a Limited Distributed system) as well as more highly permeable fractures and faults that contribute major feedzones and high productivity.

Relatively fewer stratigraphic systems have been characterized, with MPWPIs ranging from 0.1 to 8.4 kg/s/bar and a median of 1.2 kg/s/bar. Four of the systems characterized are from sandstone dominated reservoirs in the Imperial Valley region of the United States and from Cerro Prieto in neighboring Mexico. Other examples of stratigraphic reservoirs globally would include deep basin systems such as DEEP in Saskatechwan, Velika Ciglena in Croatia, and systems in the Upper Rhine Valley, Germany. The matrix permeability of stratigraphic systems, especially those hosted in siliclastic sequences, is expected to decrease with increasing depth due to compaction and diagenetic processes, which leads to generally lower PIs in systems where the heat source is primarily conductive, compared to higher PIs in the Imperial Valley type systems where convective heat transfer elevates the temperatures of shallow sandbodies, with characteristic PIs in the range 5 to 10 kg/s/bar. Of the systems characterized, both Heber and the Salton Sea could be further characterized as hybrid Stratigraphic-Enhanced Distributed systems (Libbey and Murphy, 2026), with background permeability consisting of porous matrix (rather than distributed fractures), and some producers encountering fracture or fault permeability which contribute to higher PIs.

Table 1: Summary of Reservoir Engineering Characteristics of Permeability Regimes

Permeability Regime	Median of Field MPWPIs (kg/s/bar)	Average of Field MPWPIs (kg/s/bar)	Range of Field MPWPIs (kg/s/bar)	Median of Field Average KHs (D-m)	Range of Field Average KHs (D-m)	Observed Average Temp. Decline (°C/year)	Average Temp. Decline (°C/year) Normalized for 500 kg/s Flow
Discrete	**39**	**77**	**7.1 - 377**	**124**	**17.5 - 323**	**-1.3**	**-1.5**
Limited Distributed	**1.6**	**1.7**	**0.5 - 3.45**	**6.4**	**1.2 - 80.3**	**-0.7**	**-1.2**
Enhanced Distributed	**14.5**	**130.9**	**5 - 1500**	**106**	**2.6 - 2621**	**-0.8**	**-0.3**
Stratigraphic	**1.2**	**2.8**	**0.1 - 8.4**	**29**	**0.1 - 92.5**	**-0.5**	**-0.4**

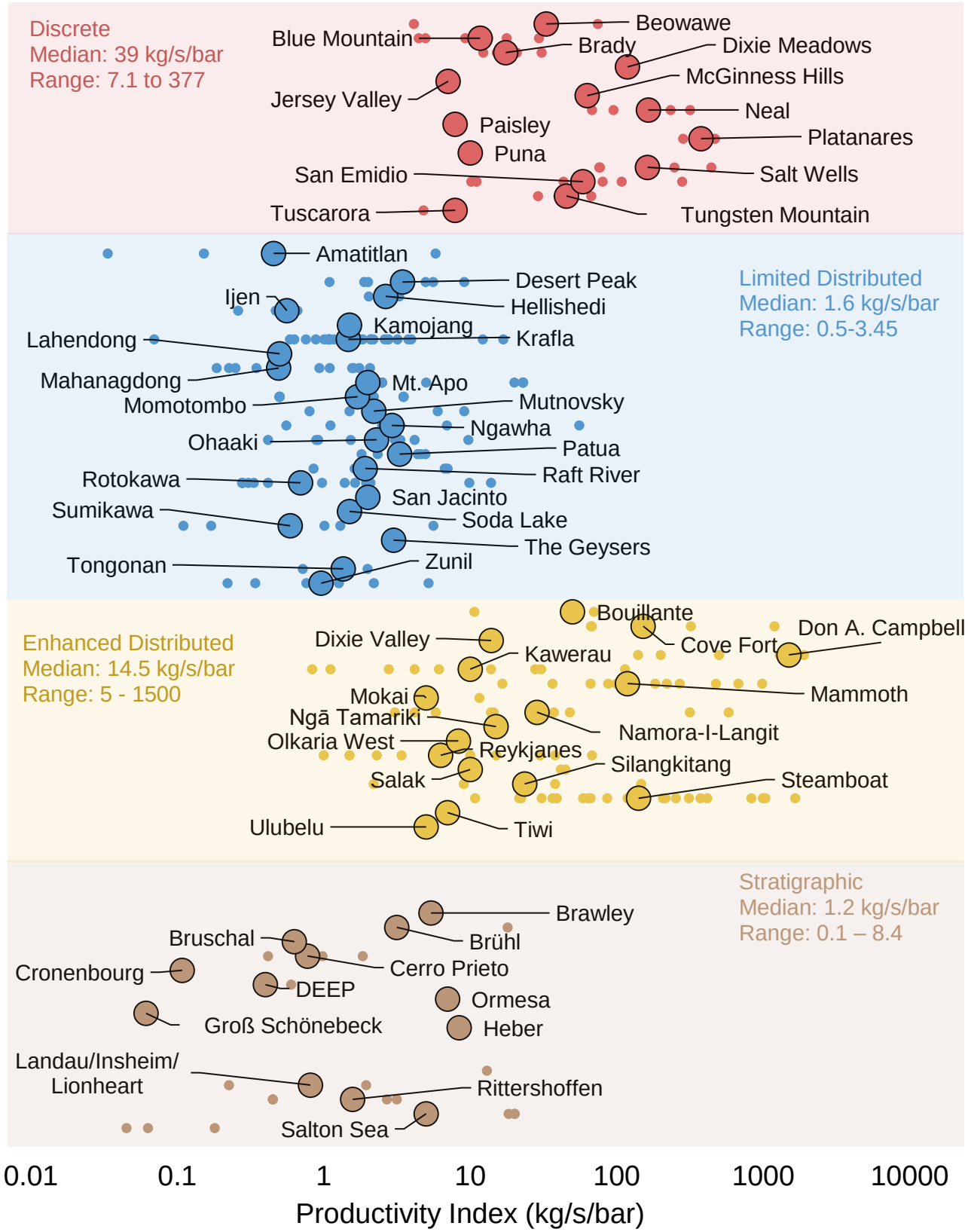

Figure 2: Median Production Well PI for Characterized Fields as Large Markers, Individual Wells as Smaller Markers

3. FEEDZONE DISTRIBUTION

The distribution of feedzones helps to further characterize permeability regimes. Feedzones are identified through a comprehensive use of flowing pressure/temperature/spinner surveys, image log analysis, and drilling indicators (such as lost circulation), and are described for calibration analog fields of each permeability regime herein.

3.1 Discrete System Feedzone Characteristics

Feedzones in a Discrete System are characterized by distinctive zones of permeability within a well, with negligible permeability between those feedzones. Feedzone interpretations from a typical well in a Discrete Permeability Regime (18A-21 at the San Emidio field) is shown below in Figure 3. A fault zone is encountered from 575 to 600 meters MD, aligning with two planar fractures observed in image logs. Spinner data shows noisy behavior above this feedzone, but the temperature signal shows no indications of additional inflows. This single feedzone is associated with very high permeability (250 kg/s/bar). The associated conceptual model is also shown, with the feedzones interpreted as intersecting the Lake Range Fault.

A second example is shown from well BCH-2 at the Brady geothermal field. This well was not a producer, but has been used as an observation well throughout the field history. Throughout its operating history, production temperatures at Brady have declined from 180+ to 120 °C as a result of injection breakthrough. Well BCH-2 crosses a fault zone which is a primary conduit for fluid flow in the system. Temperature surveys collected at 6 and 26 years after plant startup show the cooled, discrete fault zone from 550 to 810 meters depth, a wide zone surrounding a discrete permeability feature identified by total losses at 647 m.

Geologically, the permeable targets in Discrete networks may be well constrained, such as at the Tungsten Mountain field where directional drilling has been employed to repeatedly cross the targeted sub-planar fracture (Delwiche et al, 2018)

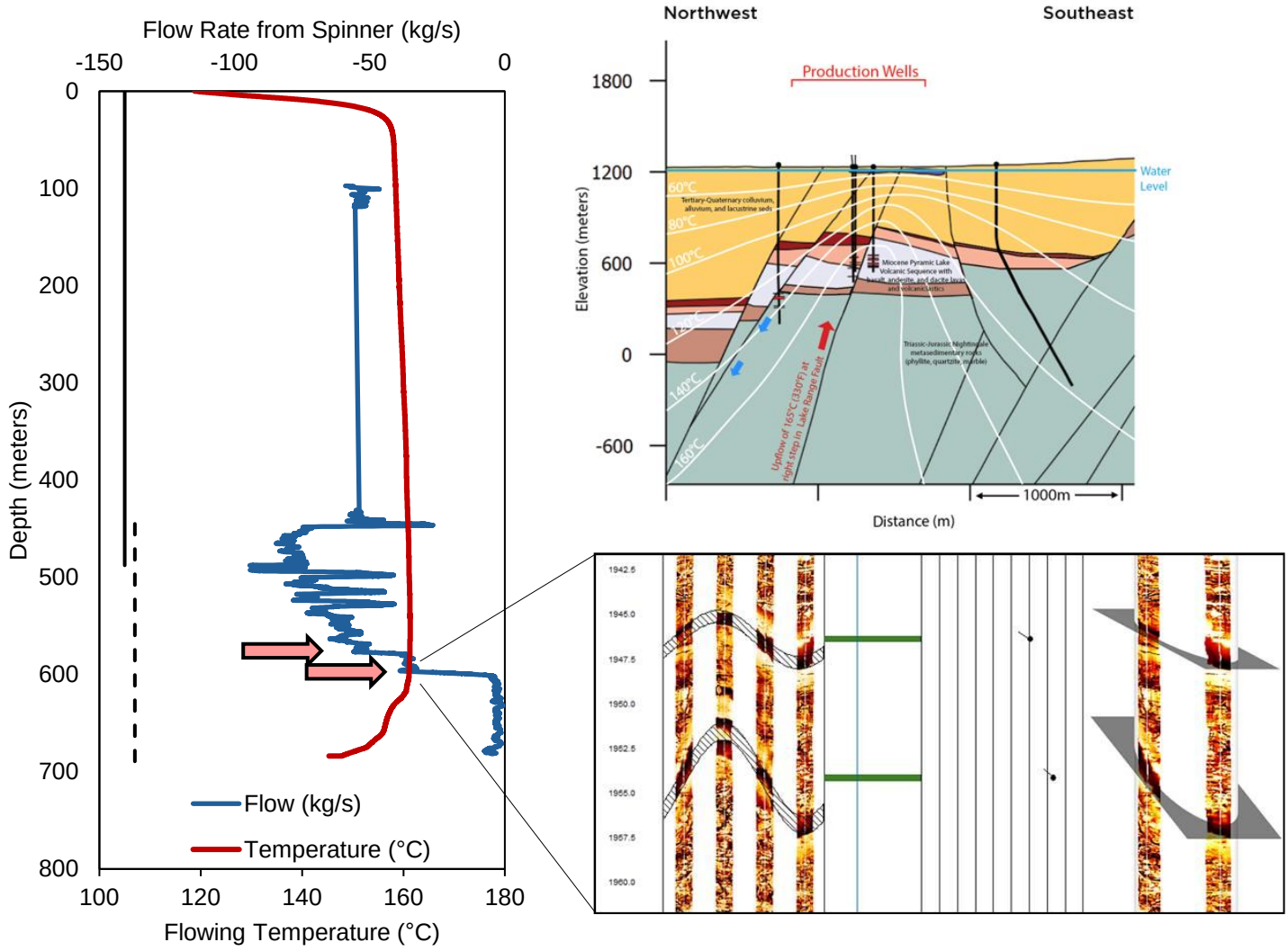

Figure 3: San Emidio 18A-21 Feedzone Analysis

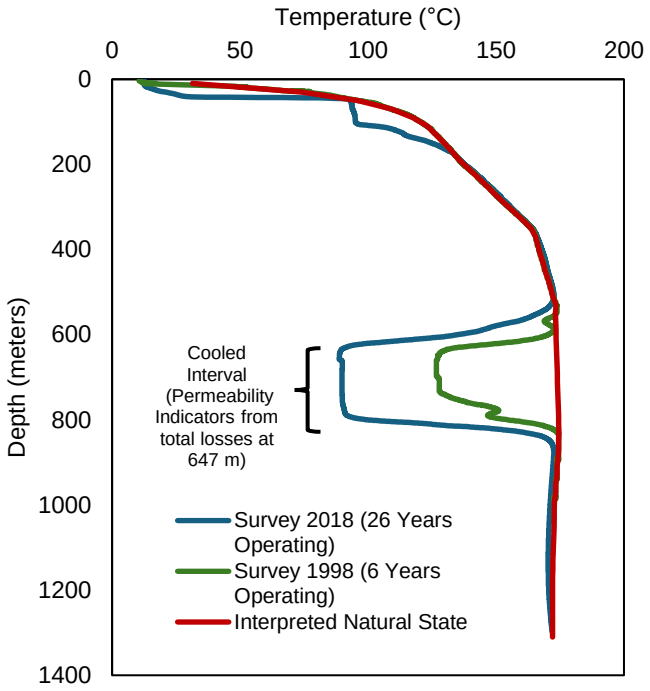

Figure 4: Brady BCH-2 Temperature Profiles at Natural State, 6 Years, and 26 years of Operations

3.2 Limited Distributed System Feedzone Characteristics

Wells in Limited Distributed systems typically encounter several minor feedzones which contribute to a cumulative PI less than 5 kg/s/bar. A typical example comes from the Zunil field in Guatemala; well ZCQ-3 produces from a liquid reservoir with three zones of inflow identified from spinner analysis and the flowing temperature profile, as shown in Figure 5. Despite the 330-meter-thick section of permeability, the total PI is only 5 kg/s/bar, the highest encountered at the Zunil field, with other producers ranging from 0.2 to 2.2 kg/s/bar.

A second example is well IJN5-1 at the Ijen field in Java, Indonesia (Libbey et al 2026), shown in Figure 6. In this case, an injecting spinner log is used to identify feedzones and many fractures were identified from analysis of an image log. This well encountered a thick, distributed feedzone from 1700 to 2400 meters, contributing approximately 70% of the permeability. A more highly fractured interval below 2400 contributes the remaining 30%. Despite this thick section of permeability evident in IJN5-1 and most wells at Ijen, the median PI is 0.6 kg/s/bar, typifying a Limited Distributed system.

In the Great Basin, the Patua field in Nevada, USA is an example of a Limited Distributed system, which is characterized by a large area but low permeability, inferred to have a median of 3-4 kg/s/bar from reported well flow rates (NDOM, 2026). Patua produces from a granodiorite that is describe as “extensively fractured”, but feedzones are predominantly from a “few large fractures”, associated conceptually with SSW-NNE striking fault zones (Cladouhos et al, 2015). This fault-associated permeability is differentiated from Discrete systems due to the lower individual well permeability and the existence of an extensive thermal anomaly (mean of 7.7 km^2, Libbey and Murphy 2026) throughout the fractured granodiorite.

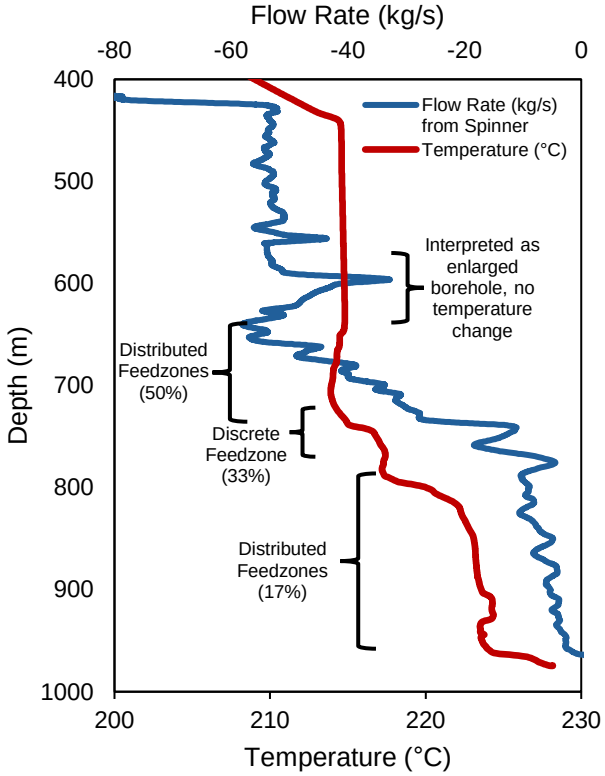

Figure 6: Zunil ZCQ-3 Flowing from Spinner and Temperature

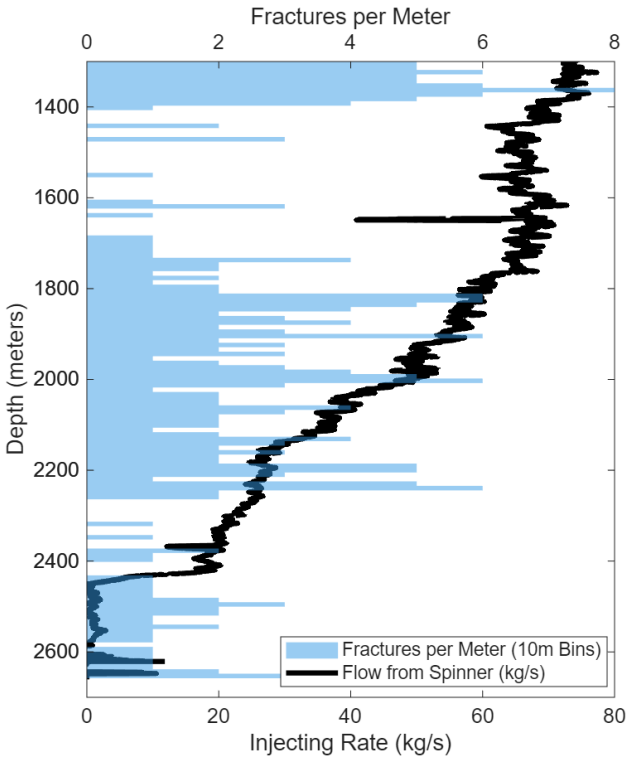

Figure 5: Ijen IJN5-1 Spinner Log and Fracture Analysis

3.3 Enhanced Distributed System Feedzone Characteristics

Enhanced Distributed systems are characterized by sections of distributed permeability, with some individual fractures or faults contributing to higher permeability (greater than 5 kg/s/bar total). The Mammoth field in California, USA provides one example of the feedzone distribution in an Enhanced Distributed. Figure 7 shows the spinner analysis and flowing temperature profile from wells 14C-25. Geologically, these wells primarily target a NW trending, steeply dipping fault zone, but also drill through the heavily fractured Bishop Tuff. In 14C-25, the primary fault is encountered at 715 meters and represents the dominant inflow, but the spinner analysis and temperature profile shows gradual inflows from 600 to 700 meters throughout the fractured Bishop Tuff. The total PI of 14C-25 is 18 kg/s/bar and neighboring 14B-25 has a PI of 67 kg/s/bar from similar permeable features.

Olkaria West in Kenya provides another example of an Enhanced Distributed system. An injecting temperature profile shown in Figure 8 shows feedzones distributed from 1857 to 2733 meters, collected during an injection test which measured an injectivity of 20 kg/s/bar. While flowing, Well A has produced up to 160 kg/s at 1220 kJ/kg with a calculated PI of 9 kg/s/bar. Feedzones in the Olkaria West are associated with rift-zone parallel fractures and features associated with the cross-cutting Olkaria Fault Zone. Wells which do not encounter major fault zones may have low PIs (0.5 to 3 kg/s/bar, representing Limited Distributed permeability), but several producers including Well A produce from larger fault zones with PIs up to 40 kg/s/bar. Olkaria West Well B (Figure 8) shows a cooling profile similar to Brady BCH-2, with primary permeable zones evident as zones of increased injection breakthrough. A 2022 flowing temperature survey shows two sharply cooled zones at 1300 and 1370 meters depth and a static survey in 2025 confirms a roughly 100-meter cooled zone above 1310 meters depth. Similar behavior was observed in the first decade of production at Tiwi, another Enhanced Distributed system, with a single feedzone cooling at a rate of ~10 °C/year (Nag-4, Barker et al 1990).

The Ulubelu field in Sumatra, Indonesia is a third example of an Enhanced Distributed system or on the high end of Limited Distributed permeability, inferred from the total generation and number of production well which indicate an average flow over 95 kg/s per producer at plant startup and an average PI from 4 to 6 kg/s/bar estimated using wellbore modeling. Ulubelu also has evidence for high permeability in individual wells, such as UBL-DL5 with a total flow > 200 kg/s during well testing and 168 kg/s during operations, and UBL-JL3 which exceeded 220 kg/s total flow, both indicating PIs exceeding 10 kg/s/bar (Yuniar et al, 2015, Sugiharto et al 2021). Arifin et al (2021) provides a detailed characterization of the mix of minor and major feedzones, with dominant feedzones contributing 30-80% over 10-100 meter thick zones, and minor zones as low as 5% being identified throughout the wells. Through image log and conceptual model interpretation, feedzones contributing over 40% are associated with faults, primarily in a NW-SE orientation. At Ulubelu, the rhyolitic tuff reservoir unit is inferred to provide both bulk permeability and host discrete zones.

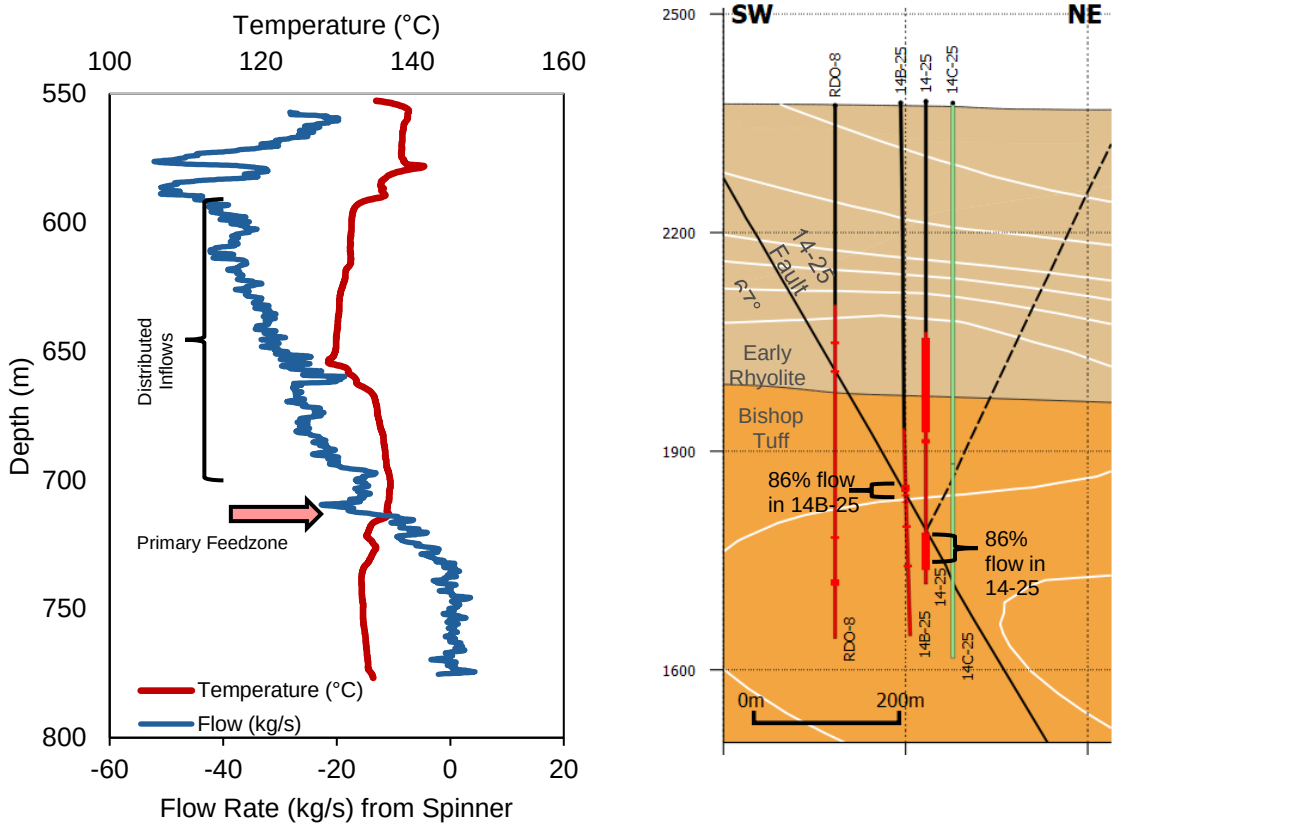

Figure 7: Feedzone Interpretation in Mammoth 14C-25 (Temperature from Testing, Heated to 163 °C)

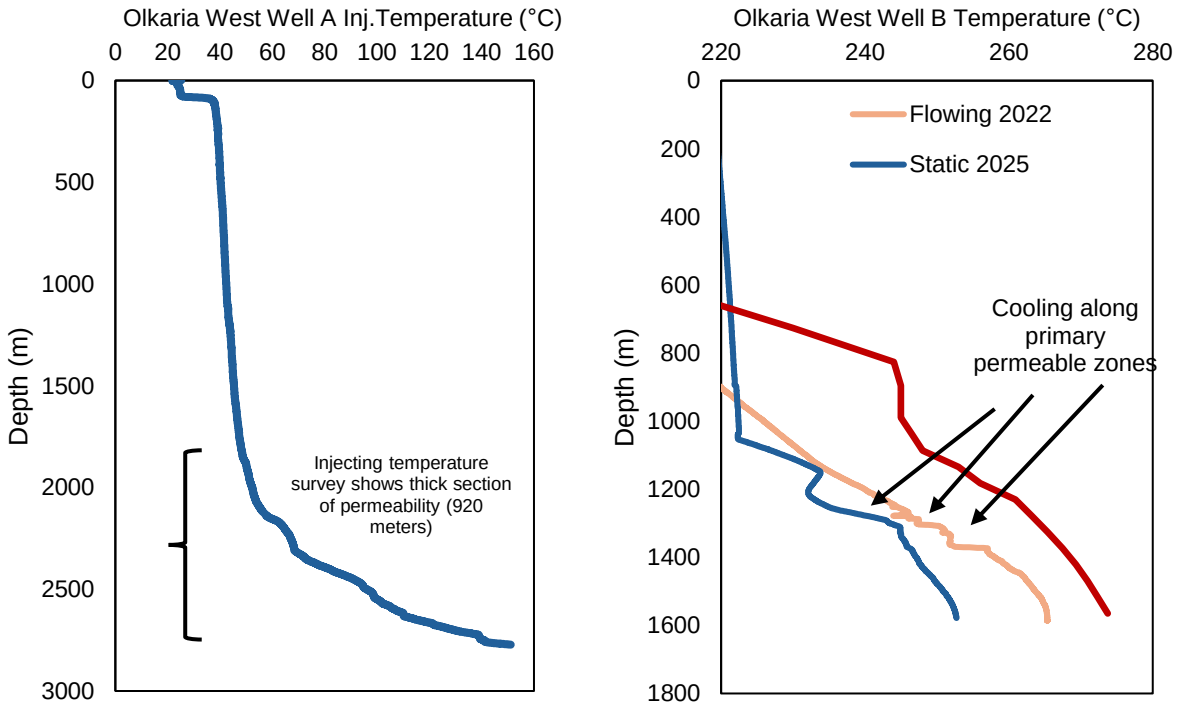

Figure 8: Feedzone and Cooling Pathway Evidence from Olkaria West

3.4 Stratigraphic System Feedzone Characteristics

Stratigraphic systems are characterized by distributed feedzones associated with primary permeability in porous formations. The Heber Field in the Imperial Valley, USA provides a typical example. A spinner analysis from injector HGU-255 is shown in Figure 9, showing a distributed zone of feedzones from 918 to 2000 meters. Shown at right is the Net Reservoir, a combined parameter described in Ramirez et al (2023) characterizing potential flow units. A flow zone from 1000 to 1100 meters depth contributes ~40% of the injection capacity and is associated with very high Net-to-Gross, bed thickness, and reservoir quality (Net Reservoir) resulting in the high permeability of this zone. HGU-255 encounters additional permeable zones contributing the remaining 60% of injectivity occurring through the thick reservoir from 1100 to 2000 meters depth. The total injectivity index of this well is 4.5 kg/s/bar, and would have an anticipated PI of approximately the same value using typical ratios from Heber. Figure 10 shows a second example from Ormesa, which has, in general comparatively thinner feedzones than Heber, but can host comparable or higher PIs owing to reservoir continuity and quality.

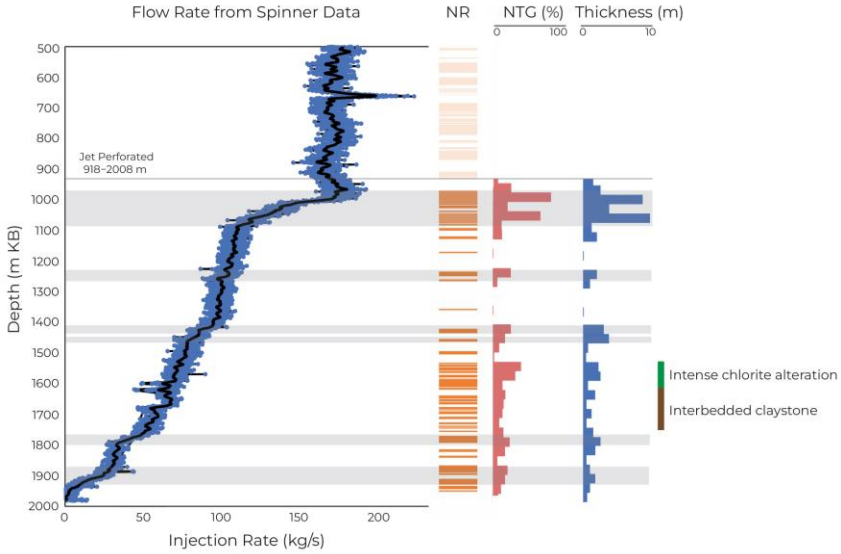

Figure 9: Injecting Spinner Profile and Sand Body Analysis from Heber HGU-255, Reproduced from Ramirez et al 2023

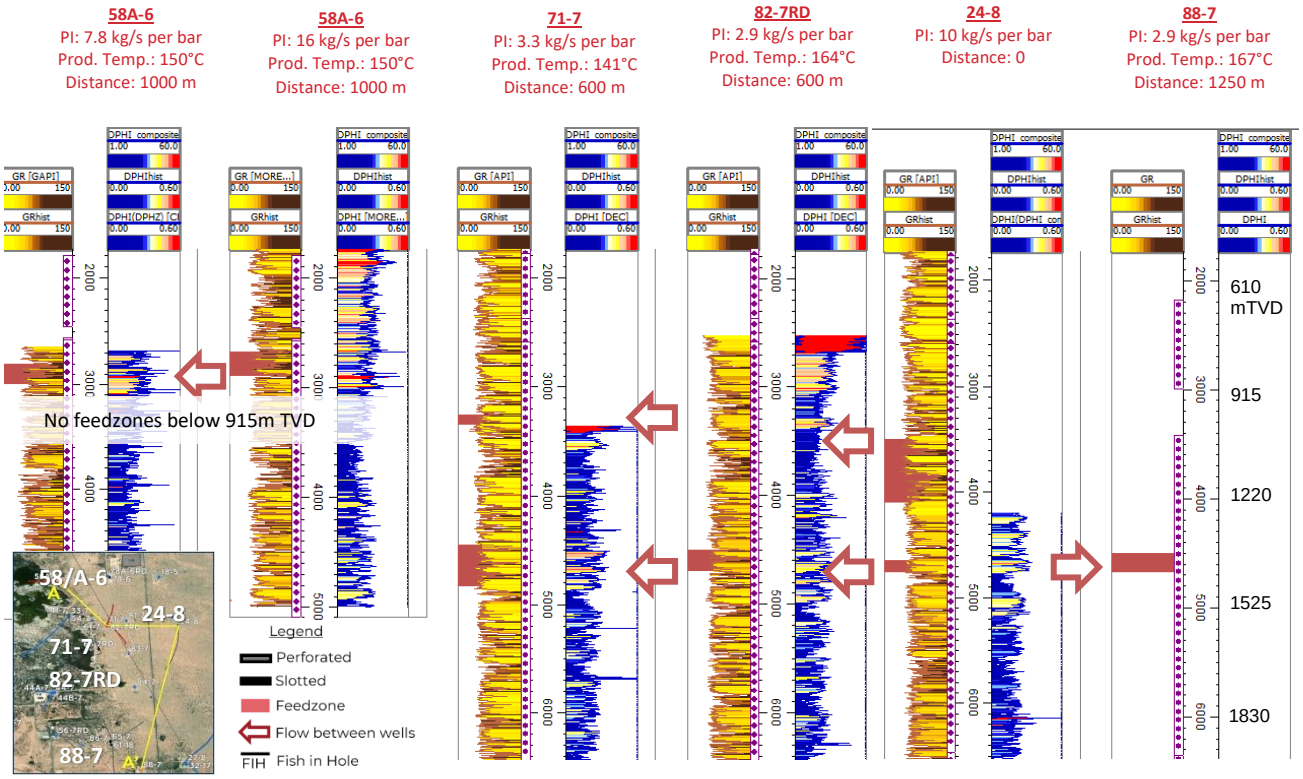

Figure 10: Correlation of Flow Zones from Interpreted Feedzones, Gamma Ray and Density-Porosity Logs for Select Wells at Ormesa, California, USA (Ramirez and Araya, 2024)

4. RESERVOIR PERMEABILITY

Figure 11 summarizes available permeability thicknesses (kh) from selected fields according to their permeability regime category. Interference testing is the ideal method for characterizing kh, but a pressure transient analysis of an individual well test can also be used to calculate this parameter. Whereas PI is summarized by the median production well PI, which avoids skewing towards outlier values, kh is summarized using a field average from all available analyses. Kh is a measure of the permeability between wells and an average of tests can more appropriately summarize the total field properties. There is a limitation in fields with multiple reservoir sectors (e.g. Momotombo with a dichotomy between the primary shallow, high permeability production and deep wells with much lower permeability, Porras and Bjornsson, 2010), and a more detailed study of kh for each field could improve on the analysis herein. However, as Figure 11 shows, there is a strong relationship between permeability type, median production well PI, and average kh.

Discrete systems range from 17.5 to 320 Darcy-meters (D-m) with a median of 124 D-m for the fields characterized. Enhanced Distributed systems range from 9.6 to 2600 D-m with an median of 106 D-m, omitting an outlier with limited data at 2.6 D-m. These values demonstrate the extremely high permeability which can exist in geothermal systems, and in the case of some Enhanced Distributed systems be spread over a large area and volume.

Limited Distributed systems range from 1.2 to 80 D-m with a median of 6.4 D-m. In the case of Limited Distributed fields, the wide spread of values and few high kh values are most likely attributed (1) two-phase effects, which reduce mobility and therefore PI in otherwise high permeability formations or (2) high skin effects (or permeability plugging with mineralization or clay as was hypothesized at Patua) can cause low productivity wells in a higher permeability formation. An alternative methodology of permeability type using kh might identify these systems as Enhanced Distributed, but this study utilizes PI which are a more reliable predictor of field output, as discussed in the conclusions regarding Recovery Factor, below, and a more direct indicator of well performance.

The stratigraphic systems available for characterization range from 8 to 92.5 D-m with an average of 29 D-m omitting an outlier at 0.1 D-m. Ormesa, with a kh of 8 D-m, represents a purely stratigraphic system producing from sandstones, whereas fields such as Heber, Salton Sea, and Cerro Prieto are interpreted to have some degree of fracture-supported permeability. The Heber field has two sections which demonstrate the differing magnitudes of kh: Heber 1 which has higher productivity and an average kh of 100 D-m, with several wells producing from a combination of sandstone and fracture-hosted permeability, and Heber 2, which is immediately adjacent to the west, produces exclusively from sandstones and has a lower kh of 19 D-m. The Salton Sea field is also known to produce from both sandstones and fracture permeability (Hulen 2003), and Cerro Prieto is estimated to have a kh of 92.5 D-m from available data. These systems exist on a spectrum, therefore, having many characteristics of a Stratigraphic system but productivity and permeability which are similar to an Enhanced Distributed system. Deeper stratigraphic systems, which exist in the absence of convective heat flow have generally lower PI and would be expected to have lower kh. This holds true at Groß Schönebeck, in the North German Basin, with a kh of 0.1 D-m, whereas Rittershoffen in the Upper Rhine Valley, Germany has a published kh of 29 D-m despite a low PI of 1.6 kg/s/bar.

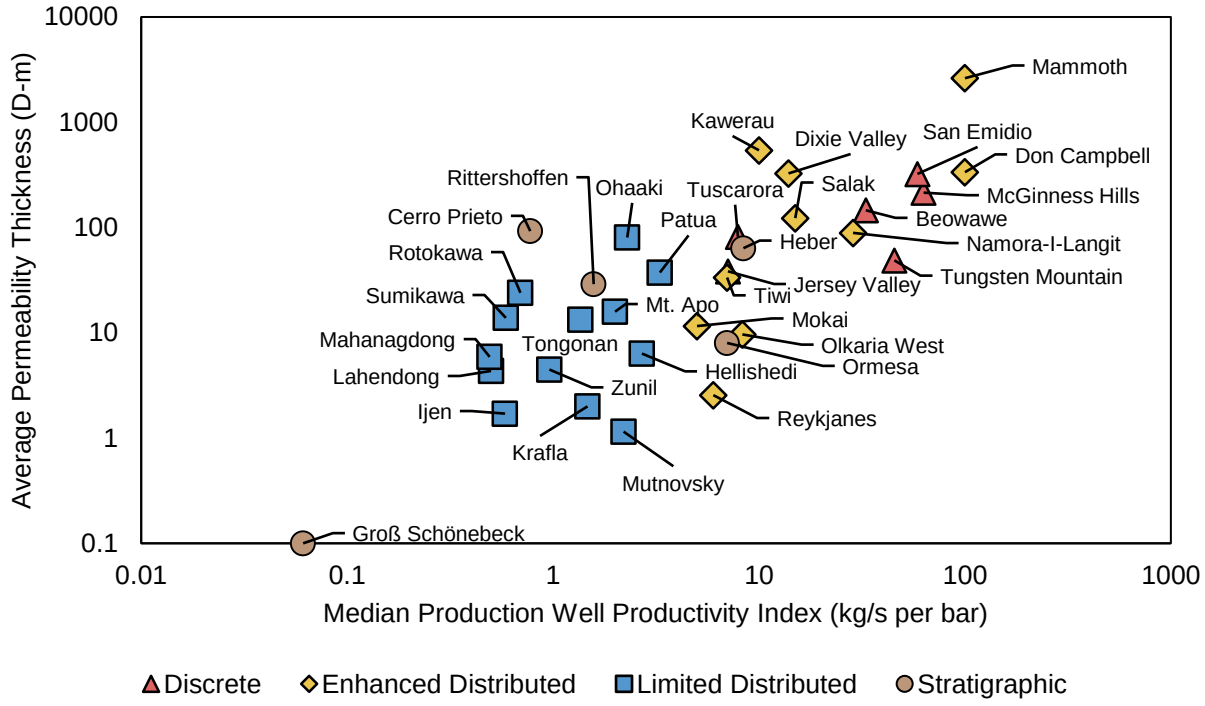

Figure 11: Average Field Permeability Thickness (kh) vs Median Production Well Productivity Index

Figure 12 depicts the pressure behavior during extended well testing of several fields, normalized to a production rate of 50 kg/s. The differing behavior of each Permeability Regime is apparent in these tests, particularly in the early-time response. Discrete and Enhanced Distributed systems are characterized by a fast pressure response associated with high permeability and an overall low magnitude of pressure decline, with McGinness Hills, Tungsten and San Emidio being most representative of a Discrete system and Don A. Campbell representing an Enhanced Distributed System. Raft River, Ijen, Patua, and Sumikawa represent limited distributed systems, with minimal response before ~1 day, but moderate magnitude by the end of the test (~1 month). In Limited Distributed systems, the monitoring pressure shown is much lower than the pressure decline in the producing well (e.g. nearly 100 bar in the producing well at Ijen). This large pressure decline is localized and does not transmit to the monitoring points due to the low permeability.

At late-time (>1 day), the pressure response of each Permeability Regime is more varied. At Tuscarora and Neal discrete systems with high MPWPIs of 7.9 and 164.5 kg/s/bar respectively, pressure decline does not stabilize after several days of production and declines similar magnitudes to lower permeability systems. At Dixie Valley, an Enhanced Distributed field with MPWPI of 13.9 kg/s/bar (and the fastest response among the fields shown, characteristic of the high permeability), the pressure decline at 1000 hours was only exceeded by Sumikawa (MPWPI of 0.59 kg/s/bar). This suggests that long-term pressure decline is less associated with individual well productivity or Permeability Regime and can be greatly affected by reservoir boundaries and the injection strategy, which has been evident in the long-term operational response of each of these fields.

At Tuscarora, pressure decline continued after the field was brought into production, a phenomenon likely related to a structural compartmentalization of the production and injection zones (Kluge et al 2025). Conversely, at Neal sufficient injection support has minimized long-term pressure decline. At Dixie Valley, the lack of pressure stabilization was noted by the developers, and injection support has proven critical at Dixie Valley (Benoit 1991, Benoit 2000). Mammoth represents a much higher permeability enhanced distributed system, as seen in Figure 13, which shows the nearly identical, extremely low magnitude monitoring response between wells at both 60 and 600 meters from a well test of well 14B-25 producing 60 kg/s. A calibrated line-source model of this behavior is best matched with the extremely high permeability thickness of 2620 D-m, the highest value found in Figure 11.

5. TRACER RESPONSE

A tracer return curve from injection to production can also be diagnostic of the Permeability Regime of a geothermal system, although the nature of a tracer response will also vary greatly depending on the inter-well distance, the presence/absence of barriers, and injection/production rates, making normalization difficult. For reference, five tracer response curves are shown in Figure 14, with concentrations normalized to 100 kg of tracer injected. The tests and well pairs were chosen to represent producers with high rates of cooling and high rates of tracer return from the injector, while choosing pairs that were generally representative of the field operating configuration. The Discrete systems show a rapid response with high concentration, with >200 ppb in <1 day at Tuscarora and 49 ppb in 8 days at Brady. Peak returns in Enhanced Distributed systems are lower and slower, 8.4 ppb at 42 days at Olkaria West and 8.9 ppb at 139 days in Dixie Valley, although faster peaks (10-30 days) were observed at Salak which motivated re-distributing injection (Acuna et al 2008).

Interestingly, returns in several limited distributed systems are similar to a Discrete network, as seen by the 83 ppb peak in 7 days at Zunil. Similar magnitudes were observed at Patua (Cladouhos et al, 2017), Desert Peak (Rose et al, 2009), and similar magnitudes but slower (30-50 day) peaks at Lahengong (Suherlina 2022). This behavior in Limited Distributed systems suggests that when background and overall permability is low, the primary fracture conduits can focus injection returns even if those fractures are low permeability compared to those observed in Discrete and Enhanced Distributed systems. As discussed in Section 6.2, the cooling observed in Limited Distributed systems is similar to Discrete systems (when normalizing for total flow rate), and Enhanced Distributed systems see generally lower cooling. This comparison on the basis of peak concentration and peak return time is limited and could be improved by comparing the magnitude of cumulative returns, which is generally more predictive of overall cooling (Silva et al 2026). No tracer study data was available for a Stratigraphic system; one tracer study was conducted at Heber but no returns were observed, suggesting that the thick sections of porous formation cause the tracer to disperse below observable limits. Should that tracer study be re-attempted, a higher mass of tracer may be necessary to generate a response.

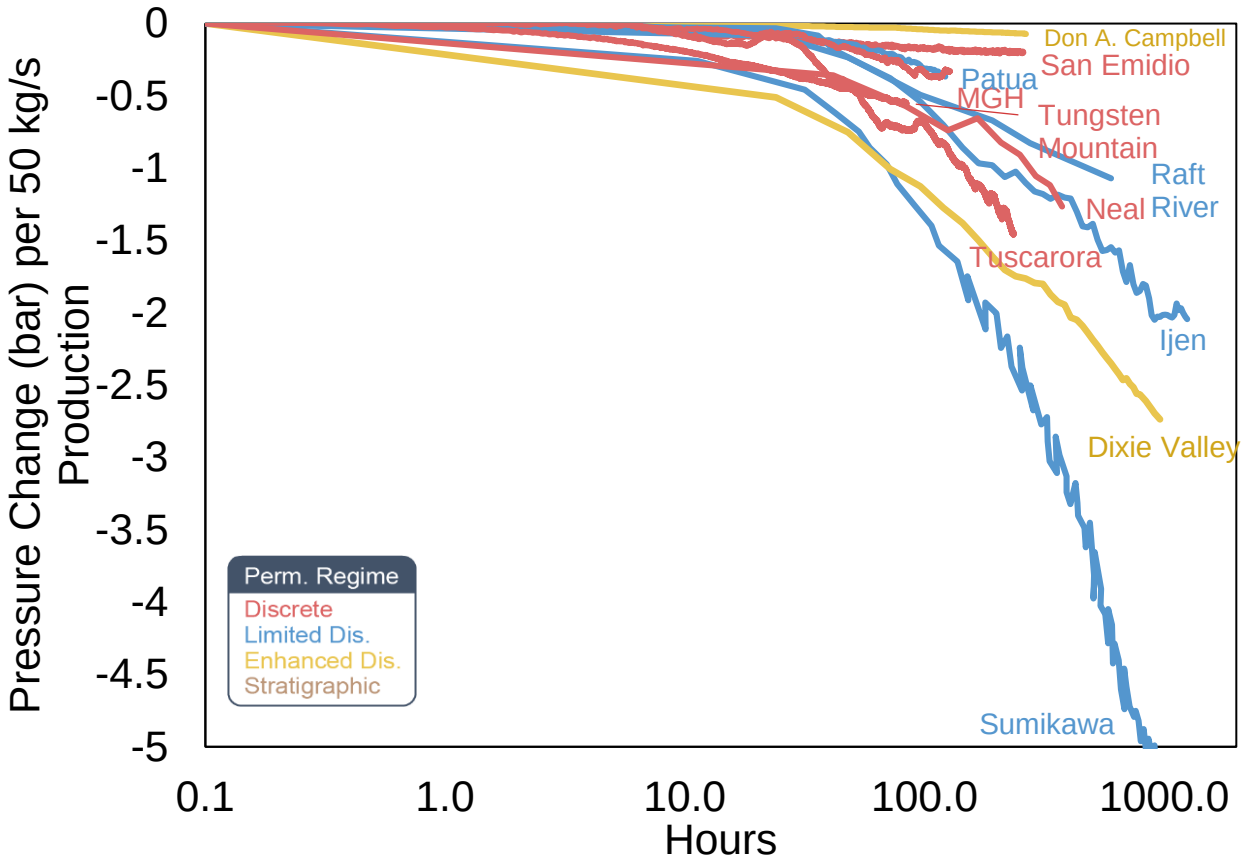

Figure 12: Pressure Depletion Behavior Normalized to 50 kg/s (Internal Data, except Patua from Combs et al 2012 and Sumikawa from Garg et al 1997)

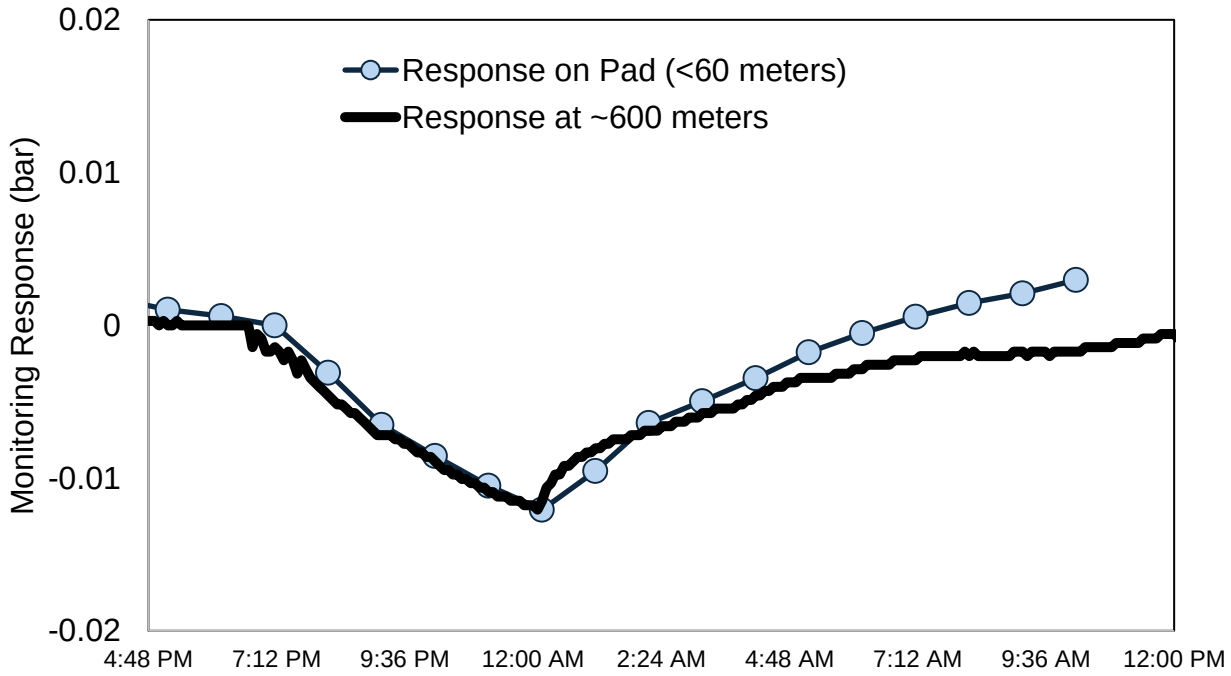

Figure 13: Mammoth (Basalt Canyon) Pressure Response during 60 kg/s Flow Test

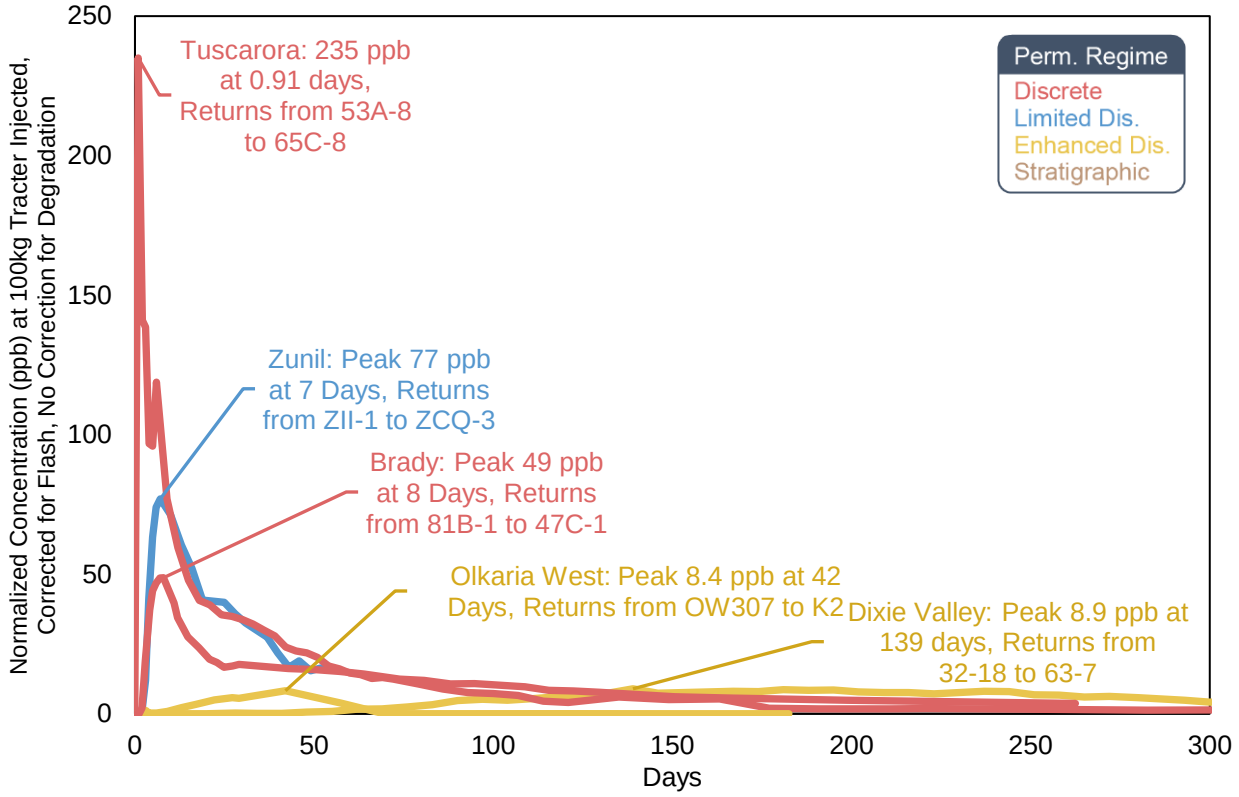

Figure 14: Representative Tracer Returns for Permeability Regimes, Normalized to 100 kg Tracer Injected and Corrected for Flash. No Adjustments made for Thermal Degradation of Tracers.

6. CONCLUSION: IMPACT OF PERMEABILITY REGIMES ON DEVELOPMENT

6.1 Well Output

The Permeability Regime of a geothermal system will have a significant impact on the likely outputs of individual wells in a field. Figure 15 shows the expected generation output per well across the four permeability regimes, an adaptation and update to a similar plot from Sanyal et al (2007). For this analysis, plant and production pump parastitics are included to provide a representative Net generation. No adjustment is made for potential injection parasitic requirements.

To calculate these outputs, reservoir assumptions include a feedzone depth of 1250 meters, water table of 100 meters below ground surface, and up to a 16” production casing for pumped wells and 13 3/8” for artesian wells. 16” production casing is common for pumped wells in Discrete or Enhanced Distributed Permeability Regimes, but is less common in artesian producers (exceptions include the successful deployment at Heber, the Salton Sea, and larger well designs implemented at Ngā Tamariki, Mak-Ban and Salak (Hulen 2003, Quinao et al 2015).

6.2 Temperature Decline

Temperature/enthalpy decline can significantly impact a field’s performance and data suggests that the proposed Permeability Regimes can predict general cooling trends of a developed geothermal field. The actual cooling observed in a field depends on the overall level of fluid throughput, injection/production spacing, and the proximity to cooler, marginal fluids, which should be considered in addition to these high-level trends.

Significant data is available from fields exhibiting liquid enthalpy, including several with over 20 years of operating history (Table 3). By virtue of their single-phase production, high-resolution temperature data is typical and is not impacted by the complexity of steam/water mixtures (excess enthalpy). Figure 16 shows the temperature behavior vs time for 23 fields exhibiting liquid enthalpy and sufficient operating history. For each field, the decline is measured from the time that field reached a representative operating configuration and flow. In addition to the absolute temperature decline, a normalized decline is shown, which is the decline multiplied by the ratio of the fields operating flow to a 500 kg/s development. Averages for each permeability regime are provided in Table 3. Discrete Permeability systems exhibit the strongest cooling (-1.3 °C/year, -1.5 °C/year normalized). In these systems, the high permeability associated with the production area may have a limited area, and finding injection outside the main producing structures is difficult. Injection may therefore return along that narrow permeable pathway. In the case of the worst cooling fields (Jersey Valley, Beowawe, and Blue Mountain), tracer returns suggest limited volume between injection and production**.** Figure 4 from Brady illustrates this narrow zone of temperature breakthrough characteristic of a Discrete system.

Limited Distributed Permeability systems cool at a similar rate when normalized (-0.7 °C/year, -1.2 °C/year normalized). In these systems, although injection could be distributed in the distal background permeability, pressure support and therefore nearby injection is required to maintain production, resulting in cooling. The tracer response curves discussed in Section 5 illustrate the similarity in injection/production connection between Discrete and Limited Distributed systems suggesting that despite the existence of background permeability, the injection returns may focus along a more focused pathway due to the overall low permeability of the system.

In Enhanced Distributed Permeability systems, the prolific permeability and large areas give good opportunities to distribute injection and minimize cooling, and the distributed fractures provide beneficial thermal recovery to the returning injectate, with an average cooling of -0.5 °C/year and -0.2 °C/year normalized). The multiple cooled zones in Olkaria West Well B (Figure 8) illustrate the spreading of returns across a thick permeable interval. Similarly, in Stratigraphic systems, cool fluids return slowly, recovering temperature in the permeable matrix, resulting in low rates of cooling (-0.5 °C/year, -0.4 °C/year normalized). Heber stands out, with an average of -0.1°C/year per 500 kg/s produced after over 30 years of producing history.

Isolating liquid enthalpy decline is difficult in high-enthalpy, self-flowing systems, because as wells decline in enthalpy they also reduce in flow or cease to flow, and total field enthalpy is apparently unchanged despite the underlying decline. At Olkaria West, some liquid zones have cooled at a rate up to 3.6 °C/year (-1.9 °C/year normalized to 500 kg/s), and a small number of wells have periodically ceased to flow to design separator pressure due to liquid enthalpy decline (generally below 235 °C, 1010 kJ/kg). Despite this cooling, overall enthalpy at Olkaria West has stayed above 1200 kJ/kg. Liquid enthalpy decline has also been cited as a cause of decline at Salak (Ganefianto et al 2010), but published data on total field enthalpy show an increasing trend in enthalpy (increasing from liquid at 1100 kJ/kg to >1800 kJ/kg overall).

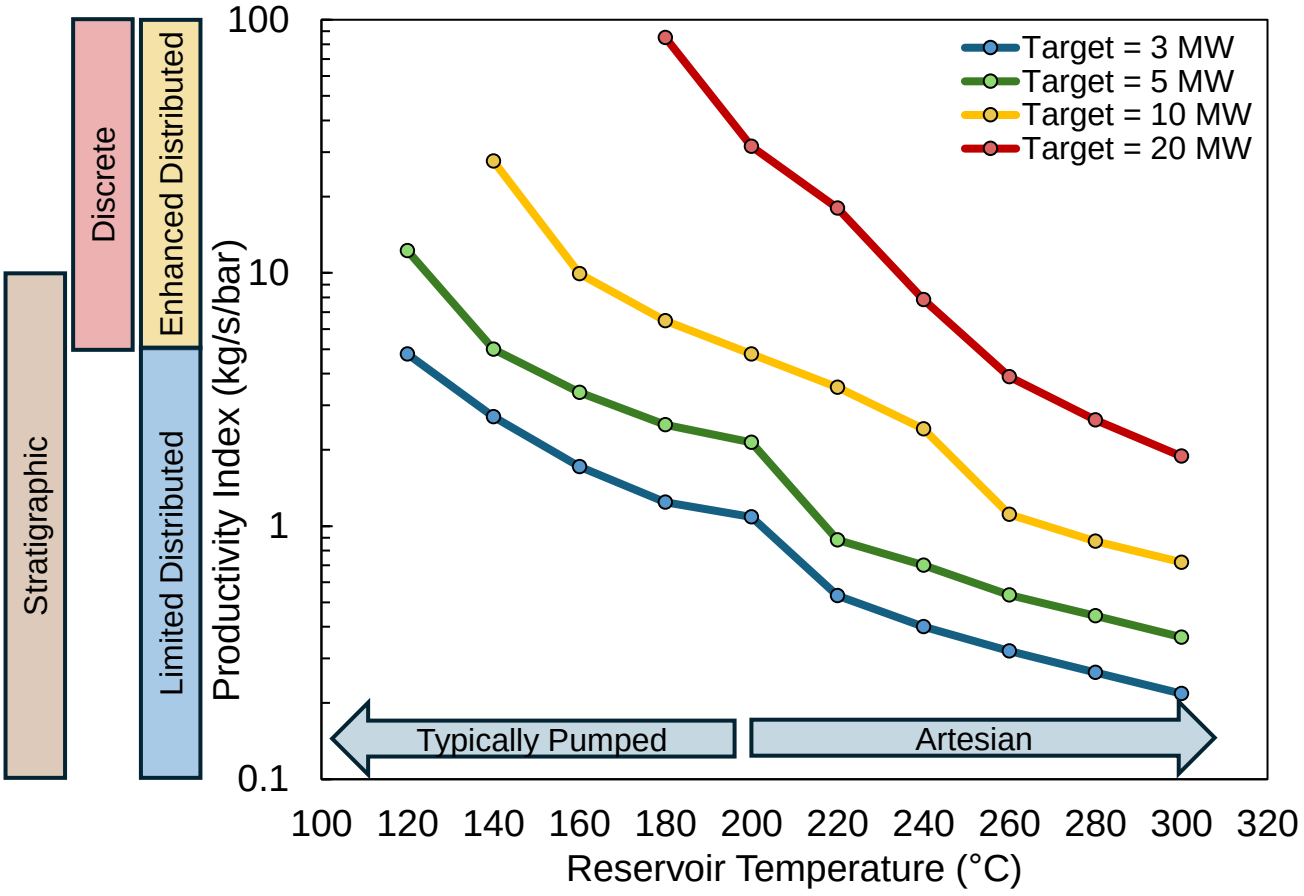

Figure 15: Productivity Index and Temperature Impact on Well Output (Net MW, Including Pump Parasitic)

Table 2: Average Temperature Decline for Permeability Regimes

Permeability Regime	Observed Temp. Decline (°C/Year)	Temperature Decline Normalized to 500 kg/s (°C/year)
Discrete Average	-1.3	-1.5
Limited Distributed Average	-0.7	-1.2
Enhanced Distributed Average	-0.8	-0.3
Stratigraphic Average	-0.5	-0.4

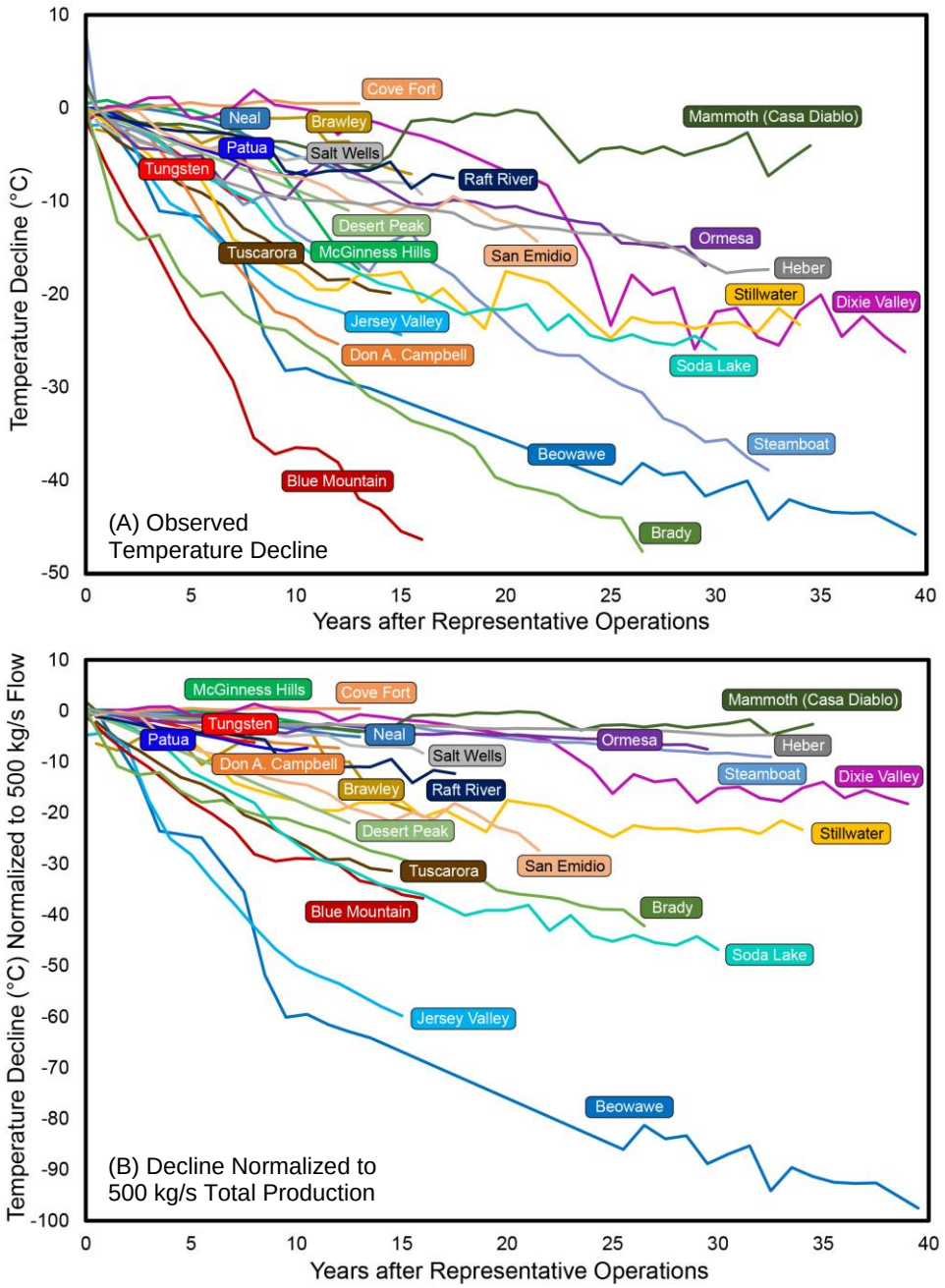

Figure 16: Temperature Decline History in Liquid Enthalpy Systems (A) Observed and (B) Normalized to 500 kg/s Flow

6.3 Recovery Factor

The concept of a recovery factor has been applied to volumetric, heat-in-place analyses of geothermal systems throughout the development history of such systems. The US Geological Survey published an early heat-in place methodology and applied it to systems throughout the United States (Nathenson, 1975a; 1975b; Nathenson and Muffler, 1975; Muffler and Cataldi, 1978; Brook, et al., 1979). Garg and Combs proposed updates to this, in particular noting the importance of utilizing field data where available (Garg and Combs, 2010) and improvements in the conversion efficiency (Garg and Combs, 2011). In 2018, Grant updated relevant recovery factors for many systems and noted the importance of a clear definition of volume, resulting in different recovery factors for "tight" and "wide" volume definitions (Grant, 2018). A method published by Standar Nasional Indonesia in 1999 establishing standards for volumetric heat-in place calculation, which utilized a recovery factor which is a function of porosity, although the few publicly available examples of this method do not provide a rigorous analysis of the relevant porosity in a fractured system and typically default to a 10% porosity and 25% recovery factor recommended in the method definition (SNI, 1999)

A detailed and well-defined method for calculating area, thickness, and reservoir temperature is provided in Libbey and Murphy, 2026. Utilizing this systematic method and calculating the 30-year power capability of developed systems allows for calculations of calibrated recovery factors for these systems. These values pertain only to the volumetric definitions as provided and are therefore not directly comparable to the recovery factors cited above or in other methods. As Grant (2018) noted, the calibrated recovery factor depends on the choice of plant parameters. To address this, the 30-year power capability uses a consistent calculation of efficiency, which depend on inlet temperature/enthalpy, ambient temperature, and injection temperature. The results of this calibration demonstrate that recovery factor is heavily influenced by both permeability type and PI. Uncertainty is inherent in heat-in-place methods, and a Monte Carlo approach is applied to uncertain parameters when determining the calibrated recovery. As shown in Figure 17, there is a clear and positive correlation between recovery factor and median production well PI. Using the diagnostic features described herein and in Libbey and Murphy, 2026, expected ranges of Recovery Factor for each permeability type can be applied, with a narrower range if the MPWPI is known.

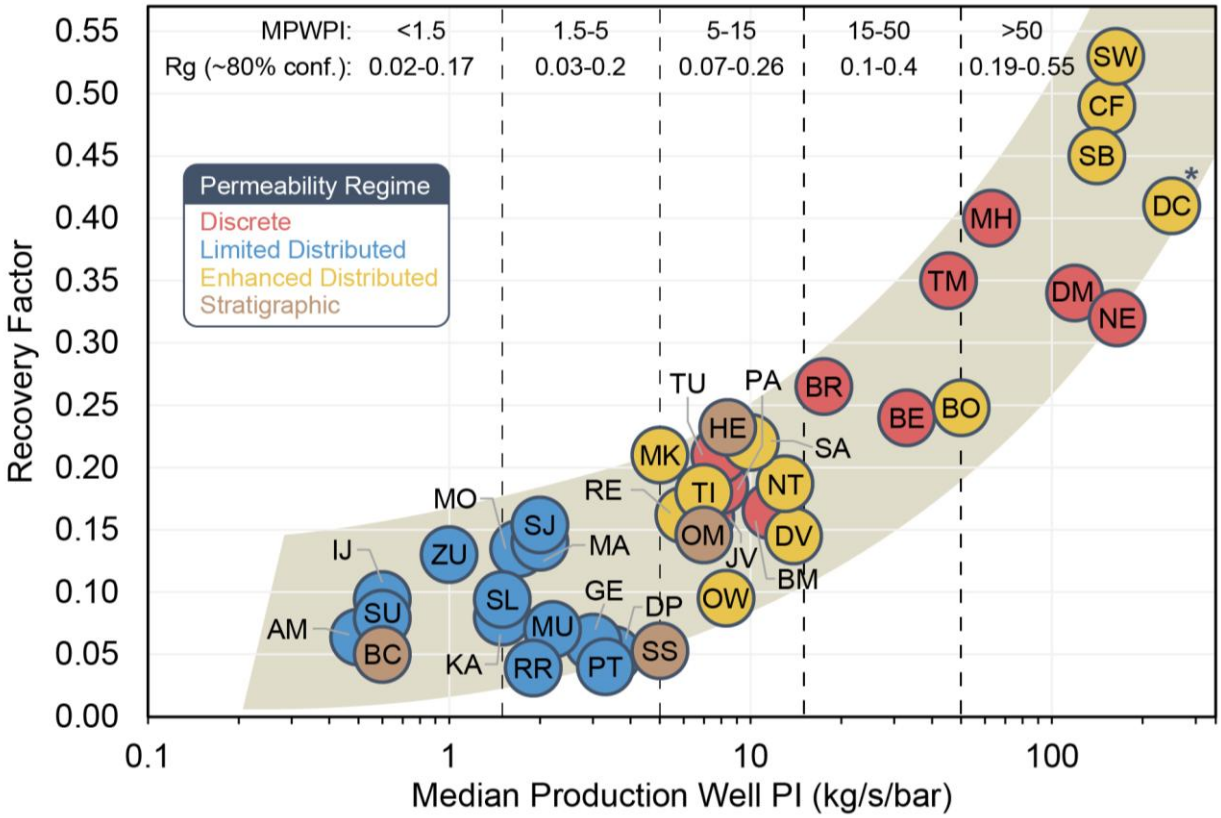

Figure 17: Recovery Factor versus MPWPI for Calibration Analogs utilized in this study. The MPWPI of Don A. Campbell is capped to 250 kg/s/bar, although data suggests this value may be >1000 kg/s/bar. See Libbey and Murphy, 2026 for the detailed methodology for calibrating and utilizing Recovery Factor.

ACKNOWLEDGEMENTS AND DISCLAIMER

The authors give a sincere thanks to Ormat, and specifically Simon Webbison, for support in publishing this paper. This study has benefited greatly from collaboration with the many talented engineers and geoscientists throughout Ormat. Additional thanks to Anthony Menzies for his review. The authors endeavored to accurately characterize the studied systems using the available data but acknowledge that many details of each system are approximate or may not accurately reflect the most up-to-date resource understanding. Support and corrections are gladly welcomed.

SUPPLEMENTARY TABLES

Table 3: Temperature Decline Summary, Individual Fields

Field Name	Permeability Regime	Temperature Decline (°C/Year)	Temperature Decline at 500 kg/s (°C/year)
Beowawe	Discrete	-1.2	-2.5
Blue Mountain	Discrete	-2.9	-2.3
Brady	Discrete	-1.8	-1.6
Jersey Valley	Discrete	-1.6	-3.9
McGinness Hills	Discrete	-1.3	-0.3
Neal	Discrete	-0.5	-0.4
Salt Wells	Discrete	-0.6	-0.5
San Emidio	Discrete	-0.7	-1.3
Stillwater	Discrete	-0.7	-0.8
Tungsten Mountain	Discrete	-1.2	-0.7
Tuscarora	Discrete	-1.4	-2.2
Desert Peak	Limited Distributed	-0.9	-1.8
Patua	Limited Distributed	-0.6	-0.7
Raft River	Limited Distributed	-0.4	-0.7
Soda Lake	Limited Distributed	-0.9	-1.6
Cove Fort	Enhanced Distributed	0.0	0.0
Dixie Valley	Enhanced Distributed	-0.7	-0.5
Don A. Campbell	Enhanced Distributed	-2.0	-0.6
Mammoth (Casa Diablo)	Enhanced Distributed	-0.1	-0.1
Steamboat	Enhanced Distributed	-1.2	-0.3
Brawley	Sedimentary	-0.5	-1.3
Ormesa	Sedimentary	-0.6	-0.3
Heber	Sedimentary	-0.5	-0.1
Salton Sea	Sedimentary	-0.3	0.0

Table 4: Productivity and Permeability-Thickness, Discrete Systems

Permeability Type	Field	Median Production Well Productivity Index (kg/s per bar)	Permeability-Thickness (D-m)	Source
Discrete	Beowawe	33.0	146.0	Internal Pump Performance, Interference Testing from Faulder et al 1997
Discrete	Blue Mountain	11.7		Internal Pump Performance
Discrete	Brady	17.5		Internal Pump Performance
Discrete	Dixie Meadows	118.6	121.9	Internal Data from Well Testing
Discrete	Jersey Valley	7.1	38.4	Internal Data from Well Tests
Discrete	McGinness Hills	63.0	214.4	Internal Data from Well Tests, Pump Performance, and Interference Testing
Discrete	Neal	164.5		Internal Pump Performance
Discrete	Paisley	7.9		Ayling et al, 2020
Discrete	Platanares	376.7		Internal Well Testing Data
Discrete	Puna	10.0	17.5	Internal Testing, kh is Post-2018 Eruption
Discrete	Salt Wells	162.5		Internal Pump Performance
Discrete	San Emidio	58.8	322.8	Internal Pump Performance and Interference Testing
Discrete	Tungsten Mountain	45.4	48.8	Internal Pump Performance and Interference Testing
Discrete	Tuscarora	7.9	81.7	Internal Pump Performance and Well Test Analysis
Discrete	Field Median	39.2	101.8	
Discrete	Field Average	77.5	123.9	
Discrete	Field Min	7.1	17.5	
Discrete	Field Max	376.7	322.8	
Discrete	Well Median	30.1	-	
Discrete	Well Average	79.7	-	
Discrete	Well Max	468.8	-	
Discrete	Well Min	4.1	-	

Table 5: Productivity and Permeability-Thickness, Limited Distributed Systems

Permeability Type	Field	Median Production Well Productivity Index (kg/s per bar)	Permeability-Thickness (D-m)	Source
Limited Distributed	Amatitlan	0.46		Internal Wellbore Model Calibration
Limited Distributed	Desert Peak	3.45		Internal Well Performance
Limited Distributed	Hellishedi	2.65	6.4	Limited Data from Wondwossen 2013, Elmi and Axelsson 2009
Limited Distributed	Ijen	0.56	1.7	Internal Well Test Analysis
Limited Distributed	Kamojang	1.50	4.9	Estimated from flow per well and internal wellbore modeling, Zuhro 2004, Sudarman et al 1995
Limited Distributed	Krafla	1.47	2.0	Landvirkjun 2015, Bovardssson et al 1984
Limited Distributed	Lahendong	0.50	4.3	Estimated from Published Well Outputs, Yani 2006, Brehme et al 2019, Fanani et al 2025
Limited Distributed	Mahanagdong	0.49	5.9	Estimations from Wellbore Simulation and Injectivity, Urmeneta 1993,Yglopaz et al 2000, Sta. Ana et al 2002
Limited Distributed	Momotombo	1.70		Estimates from Wellbore Simulation, Lopez and Ekstein 1980, Porras and Bjornsson 2010
Limited Distributed	Mt. Apo	2.00	15.9	Estimations from Wellbore Simulation, Esberto et al 1998, Molina et al 1998, Molina and Esberto 2001, Emoricha et al 2010, Malibiran et al 2013
Limited Distributed	Mutnovsky	2.20	1.2	Assaoulov 1994, Kiryukhin 2005
Limited Distributed	Ngawha	2.92		Grant et al 2013
Limited Distributed	Ohaaki	2.29	80.3	Leaver 1986, Grant et al 2013
Limited Distributed	Patua	3.30	37.3	Estimates from Public Flow Data, Nevada Department of Minerals, Combs et al 2012
Limited Distributed	Raft River	1.92		Internal Pump Performance
Limited Distributed	Rotokawa	0.69	24.0	Bush and Siega 2010, Quinoa 2013, Grant et al 2013
Limited Distributed	San Jacinto	2.00		Estimates from Per-Well Flow Rates
Limited Distributed	Soda Lake	1.50		Estimates from Public Flow Data, Nevada Department of Minerals and Ohren et al 2011
Limited Distributed	Sumikawa	0.59	13.9	Garg et al 1997
Limited Distributed	The Geysers	3.00	26.0	Estimated from flow per well and internal wellbore modeling, Enedy 2015, Faulder 1996
Limited Distributed	Tongonan	1.36	13.3	Limited Data from Abapo et al 2013
Limited Distributed	Zunil	0.96	4.5	Internal Wellbore Model Calibration and Menzies et al 1990
Limited Distributed	Field Median	1.60	6.4	
Limited Distributed	Field Average	1.70	16.1	
Limited Distributed	Field Min	0.46	1.2	
Limited Distributed	Field Max	3.45	80.3	
Limited Distributed	Well Median	1.58	-	
Limited Distributed	Well Average	3.28	-	
Limited Distributed	Well Max	55.56	-	
Limited Distributed	Well Min	0.07	-	

Table 6: Productivity and Permeability-Thickness, Enhanced Distributed Systems

Permeability Type	Field	Median Production Well Productivity Index (kg/s per bar)	Permeability-Thickness (D-m)	Source
Enhanced Distributed	Bouillante	50.0		Internal Wellbore Modeling and Well Test Analysis
Enhanced Distributed	Cove Fort	151.9		Internal Pump Performance Analysis
Enhanced Distributed	Dixie Valley	13.9	326.7	Internal Well Test Analysis and Wellbore Simulation. Limited Data for kh.
Enhanced Distributed	Don Campbell	1500.0	335.3	Internal Data from Well Testing and Interference Testing
Enhanced Distributed	Kawerau	10.0	541.7	Extrapolation from Well Performance, Burnell 1987, Bush and Siega 2010, Grant et al 2013, White and Clotworthy 2018
Enhanced Distributed	Mammoth	118.6	2621.0	Internal Pump Performance and Interference Test Analysis
Enhanced Distributed	Mokai	5.0		Published Values and Estimates from Well Performance, Grant 1985, Bush and Siega 2010, Mokai Field Consenting Documentation 2022
Enhanced Distributed	Namora-I-Langit	28.6	89.0	Internal Well Test Analysis and Wellbore Simulation
Enhanced Distributed	Ngā Tamariki	15	100	Estimated from Total Flows, Bosley et al 2010, and Ngā Tamariki Consenting Documentation
Enhanced Distributed	Olkaria West	8.3	9.6	Internal Wellbore Modeling and Well Test Analysis
Enhanced Distributed	Reykjanes	6.3	2.6	Axelsson 2006, Limited Data for kh from Rutagarama 2012 and Kajugus 2015
Enhanced Distributed	Salak	10.0	122.8	Published cumulatives adjusted for recent published drilling results, Limited kh Data, Pasikki and Gilmore 2006, ti al 2015, Libert 2017, Golla et al 2020
Enhanced Distributed	Silangkitang	23.6		Internal Well Test Analysis and Wellbore Simulation. Insufficient kh information to represent field due to high permeability.
Enhanced Distributed	Steamboat	141.1		Internal Pump Performance Analysis
Enhanced Distributed	Tiwi	7.0	33.5	Estimated from Flow Rates at Startup, Limited kh data, Barker et al 1990, Gambill and Beraquit 1993, Menzies et al 2011
Enhanced Distributed	Ulubelu	5.0		Estimated from Wellbore Simulation and flow Rate per Well, Yuniar 2015, Sugiharto et al 2021, Arifin et al 2021
Enhanced Distributed	Field Median	14.5	105.9	
Enhanced Distributed	Field Average	130.9	415.1	
Enhanced Distributed	Field Min	5.0	2.6	
Enhanced Distributed	Field Max	1500.0	2621.0	
Enhanced Distributed	Well Median	43.1	-	
Enhanced Distributed	Well Average	213.5	-	
Enhanced Distributed	Well Max	1900.0	-	
Enhanced Distributed	Well Min	0.3	-	

Table 7: Productivity and Permeability-Thickness, Stratigraphic Systems

Permeability Type	Field	Median Production Well Productivity Index (kg/s per bar)	Permeability-Thickness (D-m)	Source
Stratigraphic	Brawley	5.4		Internal Pump Performance Analysis
Stratigraphic	Brühl	3.2		Limited Data, Vidal and Genter 2018
Stratigraphic	Bruschal	0.6		Limited Data, Vidal and Genter 2018
Stratigraphic	Cerro Prieto	0.8	92.5	Arellano 1983, Shroder et al 1980
Stratigraphic	Cronenbourg	0.1		Limited Data, Vidal and Genter 2018
Stratigraphic	DEEP	0.4		Interpreted from DEEP Energy Press Release, 2020
Stratigraphic	Groß Schönebeck	0.1	0.1	Limited Data, Blöcher et al 2015
Stratigraphic	Heber	8.4	63.6	Internal Well Testing and Pump Performance, Hoang and Epperson 1984 and Faulder 1993. Note that Heber 1 kh = 100 D-m and Heber 2 kh = 19 D-m
Stratigraphic	Landau/ Insheim/ Lionheart	0.8		Vidal and Genter 2018, Vulcan Energy Press Release, 2026
Stratigraphic	Ormesa	7.0	8.0	Internal Pump Performance and Narashiman et al 1978
Stratigraphic	Rittershoffen	1.6	29.0	Limited Data, Vidal et al 2017 and Vidal 2018
Stratigraphic	Salton Sea	5.0		Extrapolated from Public Flow Data (CalGEM), Wellbore Simulation, and Siddique et al 2024
Stratigraphic	Field Median	1.2	29.0	
Stratigraphic	Field Average	2.8	38.6	
Stratigraphic	Field Min	0.1	0.1	
Stratigraphic	Field Max	8.4	92.5	
Stratigraphic	Well Median	0.7	-	
Stratigraphic	Well Average	4.7	-	
Stratigraphic	Well Max	20.1	-	
Stratigraphic	Well Min	0.1	-	

REFERENCES

Abapo, Rowena, Marie Hazel Colo, Romeo Andrino, and Edwin Alcober. 2013. "Performance Evaluation of Deepened Wells 420DA and 517DA in the Leyte Geothermal Production Field, Philippines." *Proceedings, Thirty-Eighth Workshop on Geothermal Reservoir Engineering*.

Acuña, Jorge A., James Stimac, Lutfhie Sirad-Azwar, and Riza Glorius Pasikki. 2008. “Reservoir Management at Awibengkok Geothermal Field, West Java, Indonesia.” *Geothermics* 37(3):332–46. doi:10.1016/j.geothermics.2008.02.005.

Arifin, Muhammad Tajul, Imam Muhammad Prasetyo, Vivi Dewi Mardiana Nusantara, Graniko Reza Pratama, Mochamad Husni Thamrin, and Hary Koestono. n.d. “Feed Zones Characterization Based on the Intensity of Faults and Fractures to Reduce the Uncertainty of the Future Field Development in Ulubelu Geothermal Field, Lampung, Indonesia.” *Proceedings, World Geothermal Congress 2020+1*.

Assaoulov, Stephan. 1994. “A Conceptual Model and Reservoir Assessment for the Mutnovsky Geothermal Field, Kamchatka Russia.” *UNU-GTP-1994-01. UNU Geothermal Training Programme*.

Axelsson, Gudni, Sverrir Thórhallsson, and Grímur Björnsson. 2006. “Stimulation of Geothermal Wells in Basaltic Rock in Iceland.” *ENGINE – ENhanced Geothermal Innovative Network for Europe Workshop 3, "Stimulation of Reservoir and Microseismicity*.

Ayling, Bridget F., and Nicholas H. Hinz. 2020. “Developing a Conceptual Model and Power Capacity Estimates for a Low-Temperature Geothermal Prospect with Two Chemically and Thermally Distinct Reservoir Compartments, Hawthorne, Nevada, USA.” *Geothermics* 87

Barker, B. J., P. G. Atkinson, and T. S. Powell. 1990. “Development and Production Performance of the Tiwi Field.” *Proceedings, Fifteenth Workshop on Geothermal Reservoir Engineering* SGP-TR-130.

Bauer, Johanna F., Michael Krumbholz, Silke Meier, and David C. Tanner. 2017. “Predictability of Properties of a Fractured Geothermal Reservoir: The Opportunities and Limitations of an Outcrop Analogue Study.” *Geothermal Energy* 5(1):24.

Benoit, Dick. 1992. “A Case History of Injection Through 1991 at Dixie Valley, Nevada.” *GRC Transactions* 16.

Benoit, Dick., Johnson, Stuart., Kumataka, Mark. 2000. “Development of an Injection Augmentation Program at the Dixie Valley, Nevada Geothermal Field”. *Proceedings, World Geothermal Congress, Kyushu-Tohoku, Japan.*

Blöcher, Guido, Mauro Cacace, Thomas Reinsch, and Norihiro Watanabe. 2015. “Evaluation of Three Exploitation Concepts for a Deep Geothermal System in the North German Basin.” *Computers & Geosciences* 82:120–29. doi:10.1016/j.cageo.2015.06.005.

Bodvarsson, G. S., S. Benson, O. Sigurdsson, G. K. Halldorsson, and V. Stefansson. 1981. “Analysis of Well Data from the Krafla Geothermal Field in Iceland.” *Proceedings, 7th Workshop Geothermal Reservoir Engineering* SGP-TR-55.

Boseley, Catherine, Malcolm A. Grant, John Burnell, and Brian Ricketts. 2010. “Ngatamariki Project Update.” *GRC Transactions* 34.

Brehme, Maren, Ronny Giese, Lily Suherlina, and Yustin Kamah. 2019. “Geothermal Sweetspots Identified in a Volcanic Lake Integrating Bathymetry and Fluid Chemistry.” *Scientific Reports* 9(1):16153. doi:10.1038/s41598-019-52638-z.

Brook, C.A., Mariner, R.H., Mabey, D.R., Swanson, J.R., Guffanti, M. and Muffler, L.J.P. (1979), Hydrothermal Convection Systems with Reservoir Temperatures > 90°C: in Assessment of Geothermal Resources of the United States-1978, L.J.P. Muffler, editor, *U.S. Geological Survey Circular*, 790, 170p.

Burnell, John G., and Mark J. McGuinness. 1987. “Interference Tests at Kawerau, New Zealand.” *Proceedings, Twelfth Workshop on Geothermal Reservoir Engineering* SGP-TR-109.

Bush, John., Siega, Christine. 2010. “Big Bore Well Drilling in New Zealand - A Case Study.” *Proceedings, World Geothermal Congress*

CalGEM, California Department of Conservation, Geologic Energy Management Division. *GeoSteam Web Application*. 2026. https://www.conservation.ca.gov/calgem/geothermal/geosteam.

Chiaramonte, L. 2022. “Cerro Prieto Geothermal Field: Subsurface Evaluation and Model Update—Nonproprietary Version.”

Cladouhos, Trenton T., Matt W. Uddenberg, Michael W. Swyer, Yini Nordin, and Geoff H. Garrison. 2017. “Patua Geothermal Geologic Conceptual Model.” *GRC Transactions* 41.

Combs, Jim, Neil Peterson, Sabodh K. Garg, and Colin Goranson. 2012. “Reservoir Testing and Analysis at the Patua Geothermal Federal Unit, Northwestern Nevada.” *GRC Transactions* 36.

Deep Achieves Outstanding Flow Results in Horizontal Well Test and Tom Kishchuk Appointed COO. 2020. https://deepcorp.ca/deep-achieves-outstanding-flow-results-in-horizontal-well-test-tom-kishchuk-appointed-coo/.

Delwiche, Benjamin, Brad Peters, Matt Sophy, Chandler Smith, and Jeremy O’Brien. 2018. “Successful Deployment of a Multi-Crossing Directional Drilling Method at Ormat’s New Tungsten Mountain Geothermal Field in Churchill County, Nevada.” *Proceedings, 43rd Workshop on Geothermal Reservoir Engineering* SGP-TR-213.

Elmi, Daher, and Gudni Axelsson. 2009. “Application of a Transient Wellbore Simulator to Wells HE-06 and HE-20 in the Hellisheidi Geothermal System, SW-Iceland.” *Proceedings, Thirty-Fourth Workshop on Geothermal Reservoir Engineering* SGP-TR-187.

Emoricha, E. B., J. B. Omagbon, and R. C. M. Malate. 2010. “Three Dimensional Numerical Modeling of Mindanao Geothermal Production Field, Philippines.” *Proceedings, Thirty-Fifth Workshop on Geothermal Reservoir Engineering* SGP-TR-188.

Enedy, Steven L. 2016. “Update of Augmented Injection Benefit Model of The Geysers.” *GRC Transactions* 40.

Esberto, M. B., J. B. Nogara, M. V. Daza, and Z. F. Sarmiento. 1998. “Initial Response to the Exploitation of the Mt. Apo Geothermal Reservoir, Cotabato, Philippines.” *Proceedings, Twenty-Third Workshop on Geothermal Reservoir Engineering* SGP-TR-158.

Fanani, Ahmad Fahmi, Benedict Amandus Hananto, and Dhanie Marstiga Yuniar. 2025. “Utilization Potential of Marginal Well to Maintain Steam Supply to Geothermal Power Plants: Case Study of Lahendong Field, Indonesia.” *Proceedings, 50th Workshop on Geothermal Reservoir Engineering* SGP-TR-229.

Faulder, D. D. 1993. Heber Well Test Results, Consultant Report for Ormat Energy Systems, Inc.

Faulder, D. D. 1996. *Permeability-Thickness Determination from Transient Production Response at the Southeast Geysers*. INEL--96/00182. Idaho National Engineering Lab.

Faulder, D. D., S. D. Johnson, and W. R. Benoit. 1997. “Flow and Permeability Structure of the Beowawe, Nevada Hydrothermal System.” *Proceedings, Twenty-Third Workshop on Geothermal Reservoir Engineering* SGP-TR-155.

Gambill, David T., and Domeng B. Beraquit. 1993. “Development History of the Tiwi Geothermal Field, Philippines.” *Geothermics* 22(5–6):403–16. doi:10.1016/0375-6505(93)90028-L.

Ganefianto, Novi, Jim Stimac, Luthfie Sirad Azwar, Riza Pasikki, Mauro Parini, Eri Shidartha, Aristo Joeristanto, Gregg Nordquist, and Ken Riedel. 2010. “Optimizing Production at Salak Geothermal Field, Indonesia, Through Injection Management.” *Proceedings, World Geothermal Congress 2010*.

Garg, S., J. Pritchett, J. Stevens, L. Luu, and J. Combs. 1996. *Development of a Geothermal Resource in a Fractured Volcanic Formation: Case Study of the Sumikawa Geothermal Field, Japan*. SAND--96-2556, 446314. doi:10.2172/446314.

Garg, Sabodh K., and Jim Combs. 2011. “A Reexamination of USGS Volumetric ‘Heat in Place’ Method.” *Proceedings, Thirty-Sixth Workshop on Geothermal Reservoir Engineering* SGP-TR-191.

Garg, Sabodh K., and Jim Combs. n.d. “Appropriate Use of USGS Volumetric ‘Heat in Place’ Method and Monte Carlo Calculations.”

Golla, Glenn U., Tri Julinawati, Risa P. Putri, Gregg A. Nordquist, Frederick T. Libert, and Aquardi R. Suminar. 2020. “The Salak Field, Indonesia: On to the next 20 Years of Production.” *Geothermics* 83:101715. doi:10.1016/j.geothermics.2019.101715.

Grant, M. A., and H. Barr. 1985. “Optimizing Field Proving and Development.” *Proceedings, Tenth Workshop on Geothermal Reservoir Engineering* SGP-TR-84.

Grant, Malcolm A. 2018. “Stored Heat and Recovery Factor Reviewed.” *Proceedings, 43rd Workshop on Geothermal Reservoir Engineering* SGP-TR-213.

Grant, Malcolm A., Jonathon Clearwater, Jaime Quinão, Paul F. Bixley, and Morgane Le Brun. 2013. “Thermal Stimulation of Geothermal Wells: A Review of Field Data.” *Proceedings, Thirty-Eighth Workshop on Geothermal Reservoir Engineering* SGP-TR-198.

Hanson, Hillary, Greg Mines, and Rachel Wood. 2014. “Summary of Historical Production for Nevada Binary Facilities.” *GRC Transactions* 38.

Hoang, V.T., and I.J. Epperson. 1984. Heber Well Test Reports, Internal Chevron Reports.

Hulen, Jeffrey B., Denis L. Norton, Joseph N. Moore, William Osborn, Todd van de Putte, and Dennis Kaspereit. 2003. “The Role of Sudden Dilational Fracturing in Evolution and Mineralization of the Southwestern Salton Sea Geothermal System, Imperial Valley, California.” *Proceedings, Twenty-Eighth Workshop on Geothermal Reservoir Engineering* SGP-TR-173.

Kajugus, Shakiru Idrissa. 2015. “Geothermal Reservoir Evaluation Using Well Testing and Analytical Modelling - Case Example: Reykjanes Geothermal System, SW Iceland.” *Master’s thesis, Faculty of Earth Sciences, University of Iceland*, pp. 95

Kewiy, Wondwossen Redie. 2013. “Injection and Production Well Testing in the Geothermal Fields of Southern Hengill and Reykjanes, SW-Iceland and Theistareykir, N-Iceland.” *UNU Geothermal Training Programme* 31.

Kiryukhin, Alexey. 2005. “Modeling of the Dachny Site Mutnovsky Geothermal Field (Kamchatka, Russia) in Connection with the Problem of Steam Supply for 50 MWe Power Plant.” *Proceedings, World Geothermal Congress 2005*.

Leaver, Jonathan D. 1986. “A Technical Review of Interference Testing with Application in the Ohaaki Geothermal Field.” *SGP-TR-95*.

Libbey, Ryan B., and John F. Murphy. n.d. “Standardized Definitions and Permeability Regimes for the Characterization and Capacity Estimation of Geothermal Systems.”

Libbey, Ryan, Isto Saputra, John Murphy, Munazyi Husein, Fikri Dermawan, Dalmathias Archady, Simon Webbison, Ando Deuhart, Darren Utomo, Adam Johnson, Paul Spielman, Zach Reynolds, Julfi Hadi, William Cumming, Luigi Marini, Mauro Parini, Irene Wallis, and Idham Andri Kurniawan. 2026. “Conceptual Model of the Ijen Geothermal Field, East Java: Indonesia’s First Developed Blind Geothermal System (Forthcoming).” *Proceedings, World Geothermal Contress*.

Libert, Frederick T. 2017. “Evaluation of the Deepest Production Well in Salak Geothermal Field, Indonesia.” *Proceedings, The 5th Indonesia International Geothermal Convention & Exhibition (IIGCE)*.

Lopez, Carlos V., and Yoram Eckstein. 1980. “Six Month Production Test at Momotombo, Nicaragua Preliminary Results.”

Melia, Kelly, Hyungsul Moon, Bethany Murphy, and Jamie Potter. 2022. “Resource Assessment Report.”

Menzies, Anthony J., Carla K. D. Co, and Oluwole Sotunde. 2011. "Correlation and Modeling of Reservoir Pressure Changes in the Tiwi Geothermal Field, Republic of the Philippines." *New Zealand Geothermal Workshop Proceedings*.

Menzies, Anthony J., E. E. Granados, S. K. Sanyal, L. Merida-I, and A. Caicdeo-A. 1991. "Numerical Modeling of the Initial State and Matching of Well Test Data from the Zunil Geothermal Field, Guatemala." *Proceedings, Sixteenth Workshop on Geothermal Reservoir Engineering* SGP-TR-134.

Molina, P. O., R. C. M. Malate, B. C. Buiiing, D. M. Yglopaz, J. J. C. Austria, and A. M. Lacanilao. 1998. "Productivity Analysis and Optimization of Well SK-2D Mindanao I Geothermal Project, Philippines." *Proceedings, Twenty-Third Workshop on Geothermal Reservoir Engineering* SGP-TR-158.

Molina, Patricia O., Miguel B. Esberto, Fort Bonifacio, and Patricia Molina. 2001. "Optimization Studies on Well SP-4D Mindanao Geothermal Production Field, Philippines." *Proceedings, Twenty-Sixth Workshop on Geothermal Reservoir Engineering* SGP-TR-168.

Mortensen, Annette K., Ásgrímur Guðmundsson, Benedikt Steingrímsson, Freysteinn Sigmundsson, Guðni Axelsson, Halldór Ármannsson, Héðinn Björnsson, Kristján Ágústsson, Kristján Sæmundsson, Magnús Ólafsson, Ragna Karlsdóttir, Sæunn Halldórsdóttir, and Trausti Hauksson. 2015. *The Krafla Geothermal System*. LV-2015–098. Landsvirkjun.

Muffler, L. J. P. 1978. *Assessment of the Geothermal Resources of the United States*. Circular 790. Geologic Survey.

Narasimhan, T. N., Ron C. Schroeder, Colin B. Goranson, and Sally M. Benson. 1978. "Results of Reservoir Engineering Tests, 1977, East Mesa, California." Presented at the 53rd Annual Fall Technical Conference and Exhibition of the SPE of AIME, Houston, Texas.

Nathenson, M. (1975a), "Some Reservoir Engineering Calculations for the Vapor dominated System at Larderello, Italy," *U. S.*

Geological Survey Open-File Report 75-142,47p.

Nathenson, M. (1975b), "Physical Factors Determining the Fraction of Stored Energy Recoverable from Hydrothermal Convection Systems and Conduction-Dominated Areas," *U. S. Geological Survey Open-File Report 75-525,38p.*

Nathenson, M., and Muffler, L.J.P. (1975), "Geothermal Resources in Hydrothermal Convection Systems and Conduction-Dominated

Areas: in Assessment of Geothermal Resources of the United States". D.E. White and D.L.Williams, editors, USGS Circular, **726**.

Nevada Division of Minerals Open Data Site. 2026. https://data-ndom.opendata.arcgis.com/pages/oilgasandgeothermalproduction.

Ngā Tamariki Numerical Reservoir Modelling for Supporting Consent Application. 2022.

Ohren, Mary, Dick Benoit, Mark Kumataka, and Monte Morrison. 2011. "Permeability Recovery and Enhancements in the Soda Lake Geothermal Field, Fallon, Nevada." *GRC Transactions* 35.

O'Sullivan, John, Naod Araya, Joris Popineau, Theo Renaud, and Jeremy Riffault. 2023. "A Natural State and Production Forecast Model of the Salton Sea Geothermal Field for Lithium Extraction." *GRC Transactions* 47.

Pasikki, Riza G., and Todd G. Gilmore. 2006. "Coiled Tubing Acid Stimulation: The Case of AWI 8-7 Production Well in Salak Geothermal Field, Indonesia." *Proceedings, Thirty-First Workshop on Geothermal Reservoir Engineering* SGP-TR-179.

Pasikki, Riza G., Peter, and Frederick Libert. 2017. "Impact of Enthalpy and Pressure Change to Geothermal Inflow Performance Relationship." *Proceedings The 5th Indonesia International Geothermal Convention & Exhibition (IIGCE)*.

Porras, Enrique A., and Grimur Bjornsson. 2010. "The Momotombo Reservoir Performance upon 27 Years of Exploitation." *Proceedings, World Geothermal Congress*.

Quinao, Jaime Jose, Mathew Singer, Mohsen Askari, Lutfhie Azwar, Matthew Hall, and Sunvi Ahsan. 2015. "Well Testing and Modelling of Discharging Big Bore and 'Super' Big Bore Wells." *Proceedings, World Geothermal Congress*.

Quinao, Jaime, Lutfhie Sirad-Azwar, Jonathon Clearwater, Viola Hoepfinger, and Morgane Le. 2013. "Analyses and Modelling of Reservoir Pressure Changes to Interpret the Rotokawa Geothermal Field Response to Nga Awa Purua Power Station Operation." *Proceedings, Thirty-Eighth Workshop on Geothermal Reservoir Engineering* SGP-TR-198.

Ramirez, Gabrielle, and Naod Araya. 2024. *Flow Zone Interpretation of Ormesa 24-8 and Neighboring Wells*. Internal Report.

Ramirez, Gabrielle, Robin Zuza, Adam Johnson, John Murphy, and John Akerley. 2023. "Integrated Conceptual Model of Sedimentary Basin-Hosted Geothermal Fields in Imperial Valley, CA." *GRC Transactions* 47.

Renaud, Theo, Adrian Croucher, Ken Dekkers, Michael Gravatt, Michael O'Sullivan, Joris Popineau, Jeremy Riffault, Ryan Tonkin, and John O'Sullivan. 2025. "Updated Modelling of the Salton Sea Geothermal Field." *Proceedings, 50th Workshop on Geothermal Reservoir Engineering* SGP-TR-229.

Rose, Peter, Kevin Leecaster, Peter Drakos, and Ann Robinson-Tait. 2009. "Tracer Testing at the Desert Peak EGS Project." *GRC* 33.

Rutagarama, Uwera. 2012. "The Role of Well Testing in Geothermal Resource Assessment." *Thesis, UNU Geothermal Training Programme*

Sanyal, Subir K., and Steven J. Butler. 2010. “Geothermal Power Capacity of Wells in Non-Convective Sedimentary Formations.” *Proceedings, World Geothermal Congress*.

Sanyal, Subir K., Morrow, James W., Butler, Steven J. “Net Power Capacity of Geothermal Wells Versus Reservoir Temperature – A Practical Perspective”. Proceedings, Thirty-Second Workshop on Geothermal Reservoir Engineering, 2007.

Schroeder, R. C., C. B. Goranson, S. M. Benson, and M. J. Lippmann. 1980. “Well Interference Tests at the Cerro Prieto Geothermal Field.” *Geothermics* 9(1–2):179–87. doi:10.1016/0375-6505(80)90031-0.

Siddique, Afrah K., D. D. Faulder, and Santiago Rocha. 2024. “Inferring Zonal Contributions and Productivity from a High-Temperature, High-Salinity Reservoir.” *Proceedings, 49th Workshop on Geothermal Reservoir Engineering* SGP-TR-227.

Silva, Nicholas, John Murphy, and Adam Johnson. 2026. “Application of the CSTR in Series Model on Geothermal Tracer Returns to Evaluate Long-Term Reservoir Temperature Stability.” *Proceedings, 51st Workshop on Geothermal Reservoir Engineering* SGP-TR-230.

Sta. Ana, F. X. M., C. S. Hingoyon-Siega, and R. P. Andrino. 2002. “Mahanagdong Geothermal Sector, Greater Tongonan Field, Philippines: Reservoir Evaluaton and Modelling Update.” *Proceedings, Twenty-Seventh Workshop on Geothermal Reservoir Engineering*

Standar Nasional Indonesia. 1999. *Metode Estimasi Potensi Energi Panas Bumi*. SNI 13-6171-1999.

Sudarman, S., M. Boedihardi, Kris Pudyastuti, and Bardan. 1995. “Kamojang Geothermal Field 10 Year Operation Experience.” *Proceedings, World Geothermal Congress*.

Sugiharto, Mochamad Permadi, Fadiel Evan Marastio, Ahmad Fahmi Fanani, Fernando Pasaribu, Marihot Silaban, Dimas Taha Maulana, and Nenny Miryani Saptadji. 2021. “The Implementation of Flow Performance Test to Monitor Well Performance in Geothermal Field.” *IOP Conference Series: Earth and Environmental Science* 732(1):012020. doi:10.1088/1755-1315/732/1/012020.

Suherlina, Lily, Juliet Newson, Yustin Kamah, and Maren Brehme. 2022. “The Dynamic Evolution of the Lahendong Geothermal System in North-Sulawesi, Indonesia.” *Geothermics* 105:102510. doi:10.1016/j.geothermics.2022.102510.

Urmeneta, Nemesto Noel A. 1993. *Natural State Simulation of the Mahanagdong Geothermal Sector, Leyte, Philippines*. UNU Geothermal Training Programme.

Vidal, J., A. Genter, F. Chopin. 2017. Permeable Fracture Zones in the Hard Rocks of the Geothermal Reservoir at Rittershoffen, France. *Journal of Geophysical Research: Solid Earth*. Volume 122, Issue 7, 4864-4887

Vidal, Jeanne, and Albert Genter. 2018. “Overview of Naturally Permeable Fractured Reservoirs in the Central and Southern Upper Rhine Graben: Insights from Geothermal Wells.” *Geothermics* 74:57–73. doi:10.1016/j.geothermics.2018.02.003.

Vulcan Energy reports good productivity of first well drilled for Lionheart project in Germany. 2026. https://www.thinkgeoenergy.com/vulcan-energy-reports-good-productivity-of-first-well-drilled-for-lionheart-project-in-germany/.

White, Phil, and Allan Clotworthy. 2018. “Expanding the Boundaries at Kawerau: New Data from the Te Ahi O Maui Project.” *Proceedings, 40th New Zealand Geothermal Workshop*.

Yani, Ahmad. 2006. “Numerical Modelling of the Lahendong Geothermal System, Indonesia.” *UNU Geothermal Training Programme*

Yglopaz, David, Jaime Jemuel Austria, Ramonchito Cedric Malate, Balbino Buñing, Francis Xavier Sta Ana, Reymundo Salera, and Zosimo Sarmiento. 1998. “A Large-Scale Well Stimulation Campaign at Mahanagdong Geothermal Field (Tongonan), Philippines.” *Proceedings, Twenty-Third Workshop on Geothermal Reservoir Engineering* SGP-TR-158.

Yuniar, Dhanie Marstiga, Pudyo Hastuti, and Marihot Silaban. 2015. “Ulubelu, First Year Reservoir Monitoring.” *Proceedings, World Geothermal Congress, Melbourne, Australia*.

Zuhro, Agus Aromaharmuzi. 2004. “Numerical Modeling of the Kamojang Geothermal System.” *UNU Geothermal Training Programme*